REPUBLIC OF TURKEY

ALTINBAŞ UNIVERSITY

Institute of Graduate Studies

Civil Engineering

INVESTIGATION OF POLYPROPYLENE FIBER REINFORCED BEAM BEHAVIOR ON ELASTIC FOUNDATION

Zeyd ASLAN

Master's Thesis

Supervisor

Prof. Dr. Tuncer ÇELİK

Istanbul, 2022

INVESTIGATION OF POLYPROPYLENE FIBER REINFORCED BEAM BEHAVIOR ON ELASTIC FOUNDATION

Zeyd ASLAN

CIVIL ENGINEERING

Master's Thesis

ALTINBAŞ UNIVERSITY

2022

The thesis titled INVESTIGATION OF POLYPROPYLENE FIBER REINFORCED BEAM BEHAVIOR ON ELASTIC FOUNDATION prepared by ZEYD ASLAN and submitted on 20/05/2022 has been **accepted unanimously** for the degree of Master of Science in Civil Engineering.

Prof. Dr. Tuncer ÇELİK

Supervisor

Thesis Defense Committee Members:

Prof. Dr. Tuncer ÇELİK	Faculty of Engineering and Architecture, Altınbaş Universit	____________
Prof. Dr. Zeki HASGUR	Faculty of Engineering and Architecture, Altınbaş University	____________
Asst. Prof. Dr. Erdem DAMCI	Faculty of Engineering, Istanbul University-Cerrahpasa	____________

I hereby declare that this thesis meets all format and submission requirements of a Master's thesis.

Submission date of the thesis to Institute of Graduate Studies: ___/___/___

I hereby declare that all information and data presented in this graduation project has been obtained in full accordance with academic rules and ethical conduct. I also declare all unoriginal materials and conclusions have been cited in the text and all references mentioned in the Reference List have been cited in the text, and vice versa as required by the abovementioned rules and conduct.

Zeyd ASLAN

Signature

ACKNOWLEDGEMENTS

I dedicate this work to my family and friends, and I wish to thank them for all their support, I would also like to thank my supervisor Professor Tuncer ÇELİK for his guidance.

ABSTRACT

INVESTIGATION OF POLYPROPYLENE FIBER REINFORCED BEAM BEHAVIOR ON ELASTIC FOUNDATION

Aslan, Zeyd

M.Sc., Civil Engineering, Altınbaş University,

Supervisor: Prof. Dr. Tuncer ÇELİK

Date: March/2022

Pages: 80

Polypropylene fibre reinforced beam is a new successful material in improving the behaviour of beam concrete - especially when it combines with the conventional Polypropylene reinforcement- there's an absence of codes and standard that predict and estimate the real punching capacity of the panels containing polypropylene fibre especially when it is subject on elastic foundation. Many types of reinforced concrete beams have been analysed and the solution of finite element was supported with the data from lab work. A number of parametric works were created. The influence of various key finite element and material factors, such as mesh distribution, density, and mesh size effects on the accuracy of three-dimensional finite element model outputs, was investigated. The load-deflection curves at the centre of the polypropylene fibre reinforced beam, as well as the yielding reinforcement occurrence, indicated that the behaviour of the modelled specimen may be elucidated by the load-deflection curves at the centre of the comparable traditional concrete beam.

Keywords: Polypropylene Fibre Reinforced Beam, Three-Dimension Finite Element Modelling, Meshing

TABLE OF CONTENTS

Pages

LIST OF TABLES

Pages

LIST OF FIGURES

Pages

ABBREVIATIONS

E: Elastic modulus

FE: Finite Element

RC: Reinforced Concrete

EC: Modulus of Elasticity for Concrete

ES: Modulus of Elasticity for Steel Plates

AV: Area of stirrups legs

H: Height of beam

F: Function of principal stress state (σxp, σyp, σzp)

LIST OF SYMBOLS

ft	:	Uniaxial tensile strength for concrete
fy	:	Yield stress of steel
X, Y, Z	:	Angular frequency
δ	:	Displacement
LINK180	:	3D-SPAR element 2-nodes discrete element (3 DOF per node)
SOLID 185	:	8-nodes brick element (3 DOF per node) (3 Translation DOF per node)
ε	:	Strain at stress fc
εy	:	Yield strain of steel
φ	:	Diameter of reinforcement bar (mm)
fcb	:	Ultimate biaxial compressive strength.
fs	:	The steel stress
$f1$	:	The ultimate compressive strength for a state of two-way compression superimposed on hydrostatic stress state (σha)
$f2$	:	For a condition of uniaxial compression placed over a hydrostatic stress state, the ultimate compressive strength (σha).
fn	:	Stress normal to the crack plane
Ei	:	The secant modulus
εi	;	The maximum tensile strain
fr	:	Modulus of rupture
d'	:	Depth of Compressive Reinforcement

fc' : compressive strength of concrete

v : Poisson's ratio

vC : Poisson's ratio of concrete

vs : Poisson's ratio of steel

1. INTRODUCTION

1.1 OVERVIEW

The theory of beams on elastic foundations is useful in analyzing soil-structure interaction issues, such as in building foundation engineering, railroad track foundations, pile foundations, and excavation engineering. The construction of analytical models of beams on elastic foundations has been studied in the past. The study of beam bending on an elastic basis assumes that the foundation reaction forces are proportional to the beam deflection. Equivalent, independent, discrete, linearly elastic springs define vertical deformation qualities[1]. A variety of techniques have been developed to evaluate finite beams resting on a continuous elastic media, such as power series methods, which are used to analyze finite beam issues using a power series distribution depending on the beam deflection, contact stress, and external loading[2]. The Boussinesq or Flammant solution [3] was used to determine the displacement of the earth under the beam. Another solution approach is the chain-bar method, which involves connecting the beam and the soil with a sequence of hinged rigid bars. As a result, the finite beam is transformed into a statically indeterminate structure with finite times, which may be solved using the force or displacement method. On elastic foundations, the finite element approach is also utilized to evaluate finite beams and plates[4].

The transfer matrix technique [5], the stiffness matrix method [6], the finite layer method, and the analytical layer-element method[7] have all been created to overcome boundary value difficulties in multilayered elastic materials throughout the past many decades. These methods have allowed researchers to investigate the interaction of foundations with multilayered soils.

1.2 ELASTIC FOUNDATION

A complex media, for example, a rubbery fuel binder, a fluid boundary layer, or a granular solid, is often used as the basis. At the end of the nineteenth century, the foundation's reaction at the contact area was supplied (Winkler, 1867). Under typical vertical load, the foundation is defined as a collection of closely spaced and independent elastic columns. The Winkler foundation model's basic criticism is the mutual independence of foundation columns, which leads to certain implausible findings such as uniform displacements under uniform loads, which have not been confirmed in experimental data. The Winkler foundation consists of an unlimited number of closely spaced disconnected linear springs for a more complicated medium, and is uniquely detained by the foundation modulus k. Many writers made use of finite elements. The foundation surface of the Winkler model features a displacement discontinuity between the loaded and unloaded sections, which is one of its most significant flaws. In actuality, there is no discontinuity on the soil surface (Figure 1.1) [8][9].

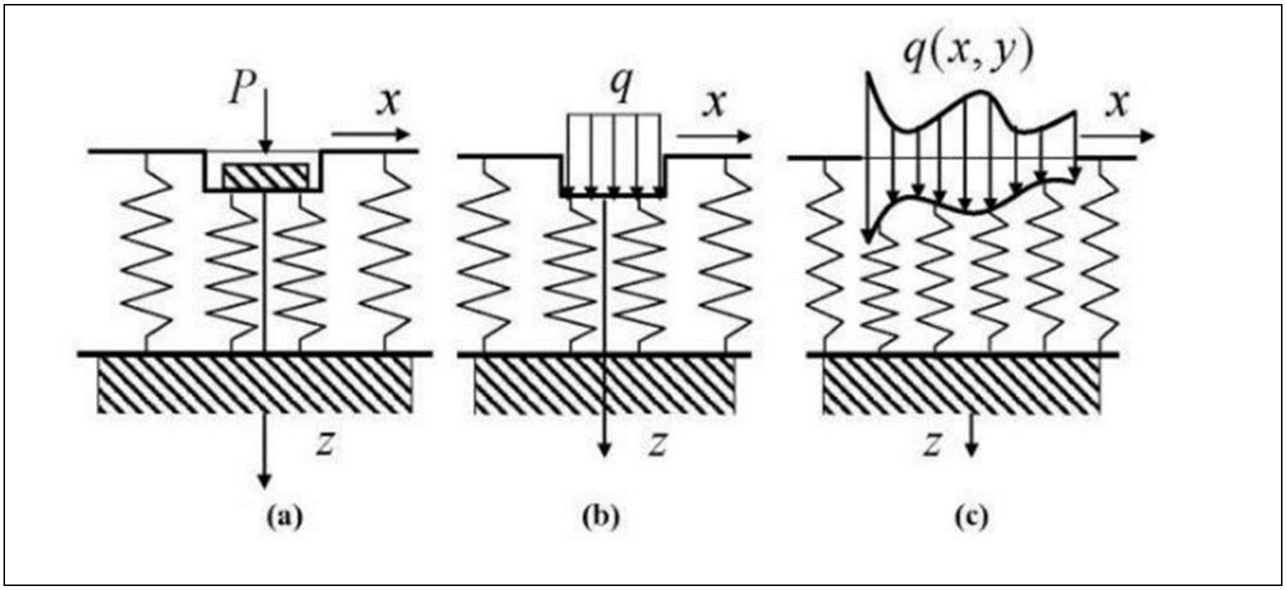

Figure 1. 1: Winkler model: (a) rigid foundation (b) flexible foundation (uniform load) (c) flexible foundation (non-uniform load)[9]

To describe the general behavior of the soil structure interface, Winkler-based techniques may employ just 1D spring elements or 1D spring elements in conjunction with 2D or 3D soil elements. Because of its simplicity and little computational effort, the Winkler spring technique is desirable in design. Furthermore, if response data is available, the mechanical character of spring-based models may make calibration easier. The effects of normal force, shear force, distributed moment, and temperature may be ignored in most cases (or the beam is not exposed to them)[6].

1.3 BEAM ON ELASTIC FOUNDATION

In case of grade beams in prefabricated buildings and combined footings for industrial beams and equipment, the member subjected to loads is supported on continuous elastic foundations such as soil or flowable fill. That is the reactions due to external loading is distributed along the length of the member. The solve of a beam on an elastic basis is a mechanical problem that is statically indeterminate as shown in figure 1.2[10][6].

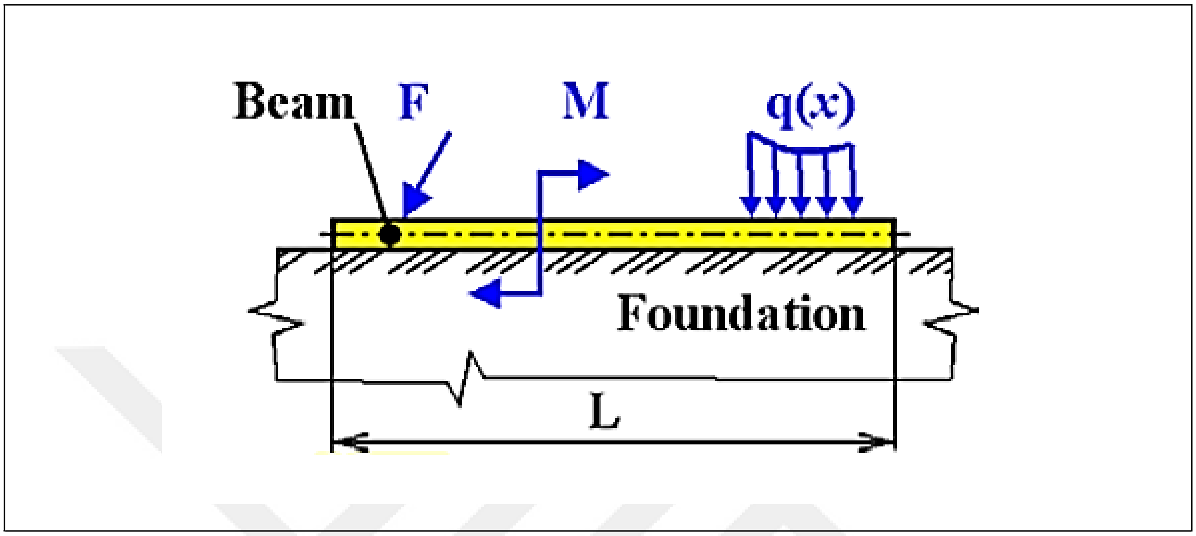

Figure 1. 2: Beam Resting on an Elastic Foundation. This beam is loaded by force F, couple M and distributed loading q[6]

In this situation, the beam has an elastic basis that runs the length and breadth of the beam or merely a portion of the length and width. Theoretical approaches cannot address all issues. The Finite Elements Method (FEM) may be used to solve these difficult situations. Ordinary differential equations represent the general issue of a beam on an elastic basis (Winkler's theory). The effects of normal force, shear force, distributed moment, and temperature may be ignored in most cases (or the beam is not exposed to them)[11][12]

$$\frac{d^4 v}{dx^4} + \frac{k}{EJ} v = \frac{q}{EI}, \qquad (1)$$

where $k = k(x)$ */Nm*$^{-2}$ */* is the foundation stiffness and, *EI /Nm2/* is the bending stiffness. An area *dA /m2/* of the foundation surface acts like a linear spring of stiffness k. The equation observes that there is a relationship between the foundation stiffness *(k)* and bending stiffness *(EI).* From this relationship, this research will highlight the differences in stiffness characteristics of concrete beam and Winkler's foundation. The general stiffness matrix presented by FRYDRÝŠEK et al, in 2013 shown in below[6]:

$$[\mathbf{K}_{bc}] = \frac{EI}{L^3}\begin{bmatrix} 12+C_M & 6L & -12 & 6L & -C_M & 0 \\ 6L & 4L^2 & -6L & 2L^2 & 0 & 0 \\ -12 & -6L & 12+C_M & -6L & 0 & -C_M \\ 6L & 2L^2 & -6L & 4L^2 & 0 & 0 \\ -C_M & 0 & 0 & 0 & C_M & 0 \\ 0 & 0 & -C_M & 0 & 0 & C_M \end{bmatrix}$$

Where C_M /1/ is the modified stiffness of spring which involves the effect of beam stiffness and Winkler's foundation.

1.4 POLYPROPYLENE FIBER REINFORCED CONCRETE

In order to enhance the concrete beam capability in foundation, the Fibers Reinforced Concrete FRC can be used. The ability of a durable structure to withstand chemical assault, weathering action, abrasion, and other degrading processes with little maintenance over the course of its service life is just as significant as the structure's ability to withstand the stresses applied to it. Although concrete has several benefits in terms of mechanical and economic elements of brittle qualities, the material's construction remains a significant disadvantage in seismic and other applications where flexibility is necessary. However, the invention of polypropylene fiber-reinforced concrete (PFRC) has recently offered a technological foundation for addressing these flaws [13]. Polypropylene is made from monomeric C3H6, a pure hydrocarbon, as its starting ingredient. Because of their kind of polymerization, Polypropylene fibers are very attractive because to their high molecular weight and the manner they are manufactured into fibers, as described below[13]:

a) The polymer molecule possesses a highly crystallinity and a sterically regular atomic arrangement. The term isotactic polypropylene refers to the material's regular structure.
b) Chemical inertness renders the fibers chemically resistant. Any chemical that isn't harmful to the concrete's ingredients will also be harmless to the fiber. Concrete will always decay first when exposed to more powerful substances.
c) Because the hydrophobic surface of the fibers is not wet by the cement paste, chopped fibers do not ball up as other fibers do during mixing.
d) Polypropylene fibers have no water need.

e) The film is brittle in the lateral direction as a result of its orientation, which promotes fibrillation. As a consequence, the cement matrix may be able to penetrate the mesh structure formed by the individual fibrils and establish a firm link.

A circular cross-section pulling wire method or a rectangular cross-section extrusion of a plastic sheet are used to create the fibers.

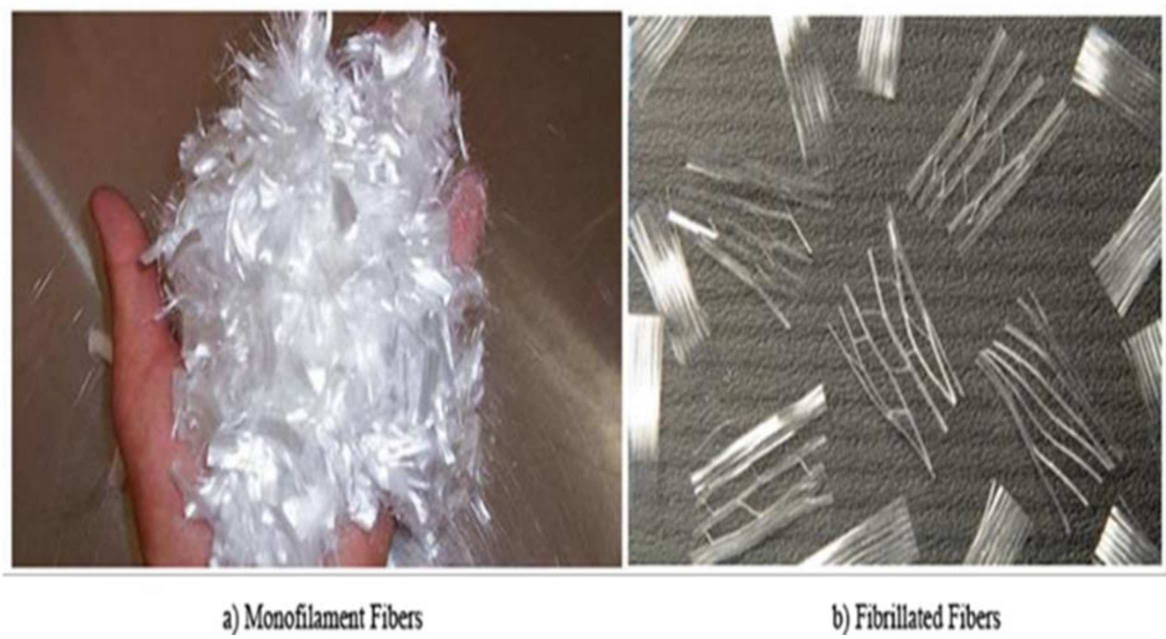

Figure 1. 3: Polypropylene Fibers [14]

The fibrillated polypropylene fibers are made by stretching a plastic sheet that is then cut into strips and sliced. The fiber bundles are fibrillated after being cut into certain lengths. The insertion of buttons to the ends of monofilament strands enhances the pullout load. Twisting fibers might potentially be used to provide maximum load and stress transmission[14].

1.5 PROBLEM STATEMENT

Beam on elastic foundation may cause a displacements and internal forces in the Winkler foundation due to the effect of subjected load. The methods for constructing beams on elastic foundations do not allow for the installation of shear and torsion reinforcement. As a result of shear and/or torsion forces, it may break without warning. Fibers have recently been used in extensive experimental research to increase the performance of beams. Synthetic fibers provide several advantages, Alkaline resistance, a high melting point, and inexpensive raw material costs are only a few of the benefits. Plastic shrinkage cracking may be reduced by using polypropylene fibers. In general, polypropylene fibers reduced the extent of shrinkage cracking, the number of cracks, maximum crack widths, and crack area. Also, crack indexes decreased significantly by adding polypropylene fibers. In real engineering conditions, there are differences regarding the control determination and the quantification of the influences of the main effective parameters. The main two problems resulting from the applied loads are brittle and high deflection. This is may occur due to the concentration of shear force and structural behavior effect which depends on the brittleness properties of concrete. There are a huge number of researches addressed this subject, but still many problems to be resolved, such as, how to increase the concrete strength and ductility at the same time and what is the relationship between the enhanced concrete and Winkler foundation.

1.6 OBJECTIVES AND SCOPES

The impact of polypropylene fiber on the residual toughness of beam subjected on elastic foundation has been experimented with. To achieve this objective, PFRC is exposed to different reinforcements are studied through the:

a) Comparison between the residual shear behavior of PFRC beam due to different fiber conditions and punching shear behavior of PFRC beam at normal conditions.
b) Investigation of the effect enhanced beam on elastic foundation.

1.7 THESIS ORGANIZATION

This thesis has five chapters. Chapter one includes an introduction to the beams and the Winkler foundation and the behavior of beam when subjected to the Winkler foundation.

Chapter two presents a general view of fibers' effects on concrete behavior in different studies collected from various researches.

The experimental program, including the studied parameters, the work methodology, and the testing of PFRC concrete specimens, are presented in Chapter three.

Chapter four discusses the result and the calculation of the work. Chapter five is the conclusion.

2. LITERATURE REVIEW

2.1 GENERAL

Many geotechnical engineering issues may be conceptualized as beams supported by elastic foundations. Soil-structure interaction processes may be better understood with the help of this sort of modeling, as well as predictions of contact pressure distribution and deformation. The Winkler technique[15], as illustrated in figure 2.1, is the most prevalent theory for beam on elastic foundation modeling.

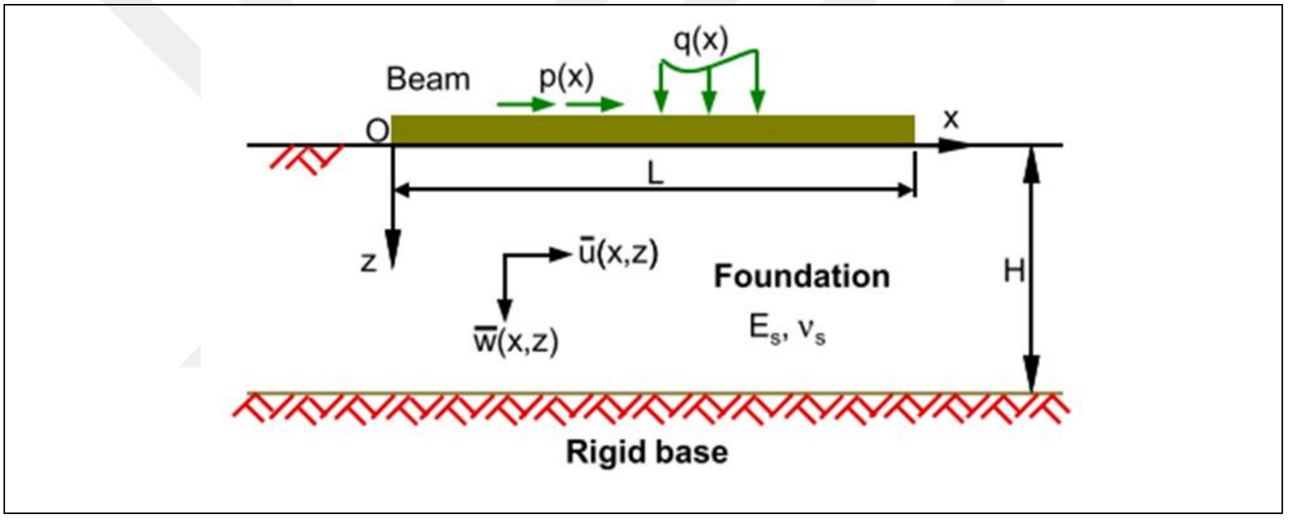

Figure 2. 1: Winkler Spring Approach[15]

The Winkler model is fairly basic; however, it does not adequately capture the properties of many real foundations. It was initially created for the examination of train lines. There is a gap in the Winkler model's foundation surface between the loaded and unloaded areas, which is one of its most significant flaws. In actuality, there is no discontinuity in the soil surface.

It has been traditional to envision a variety of linkages, such as flexural elements (such as 1-D beams, 2-D plates, shear-only layers, and distorted pretension membranes, among others) in order to overcome the deficiency of the Winkler model [16]. The Winkler model's individual spring parts are connected to an elastic membrane under constant stress in the foundation model developed in 1940 by Filonenko and Borodich[17]. An elastic plate or beam, which only deforms under bending in 3-D issues and 2-D problems, was invented by Hetényi in 1950 [1]to facilitate the interaction between spring elements. By linking the springs' ends to an incompressible vertical component that only deforms transversely, Pasternak came up with a foundation model that achieved shear interaction between springs in 1954. Two-parameter models or, more simply, mechanical models are mathematical models that incorporate a constant parameter that specifies the interaction between springs, as seen in figure 2.2 below [2].

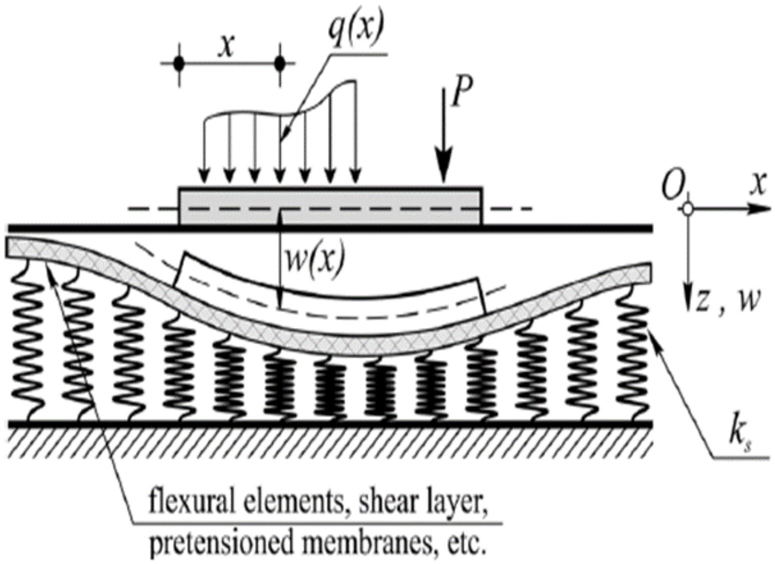

Figure 2. 2: Beam Resting on Two-Parameter Elastic Foundation[18]

2.2 EXPERIMENTAL AND ANALYTICAL RESEARCHES

Zhi Yong Ai et al. [1]examine isotropic 3D multi-layered 2D plane-strain soils with elastic foundation finite beams using boundary element analysis. It is created using basic elasticity equations and the Fourier transform for a single soil layer. The solution to multi-layered elastic soils is obtained by BEM analysis using boundary criteria and continuity requirements between two neighboring soil layers. The elastic foundation beam is modeled using the finite difference technique as a Bernoulli–Euler beam. Solution for multilayered soils resting on a beam is found using displacement and stress conditions in the coordination of the two. An elastic foundation beam rests on stratified soils seen in Figure 2.3.

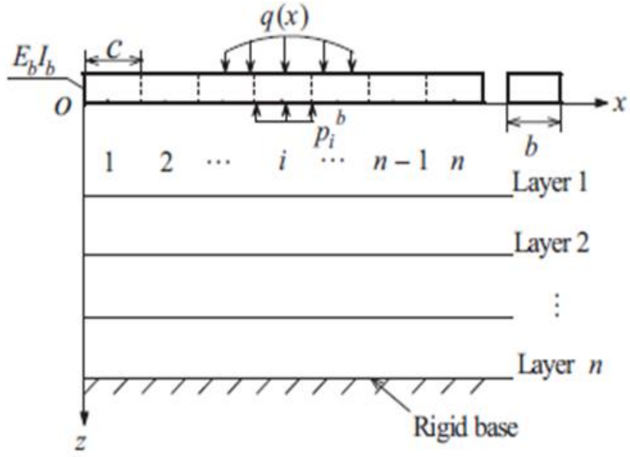

Figure 2. 3: Elastic Foundation Beam Resting on Multilayered Soils[3]

To handle the interaction issue between beams and multi-layered isotropic soils, the transfer matrix solutions for 2D plane-strain and 3D isotropic elastic media are determined and used as kernel functions of the boundary element approach.

Two numerical examples of 2D plane-strain and 3D are provided to verify the approach's accuracy, with additional examples to investigate the influence of the stiffness ratio and the stratified nature of soil on beam response. The calculations show that when the stiffness ratio between the soil and the beam grows, the settlement of the beam reduces, as do the shear stresses and moments, and that the beam becomes relatively rigid when K is less than or equal to 0.84 and flexible when K is more than or equal to 1.78. Furthermore, an examination of soil stratification reveals that soil stratification has a significant influence on the deflection and internal force of the beam, which should not be neglected.

S.M. Binesh [19] discussed a two-parameter elastic beam is investigated using radial point interpolation, a mesh-free method. They are modeled separately. To imitate a beam, place nodes on two or three parallel lines. The weak version of the governing equation is used to replace the displacement field. An elastic basis is provided by the connecting member. The foundation stiffness was investigated by calculating normal and tangential stiffness coefficients. The beam node displacement is linked to the foundation layer movement. As shown in figures 2.4 and 2.5, the whole system of equations is created by combining equations for the beam and the elastic foundation in the global coordinate system.

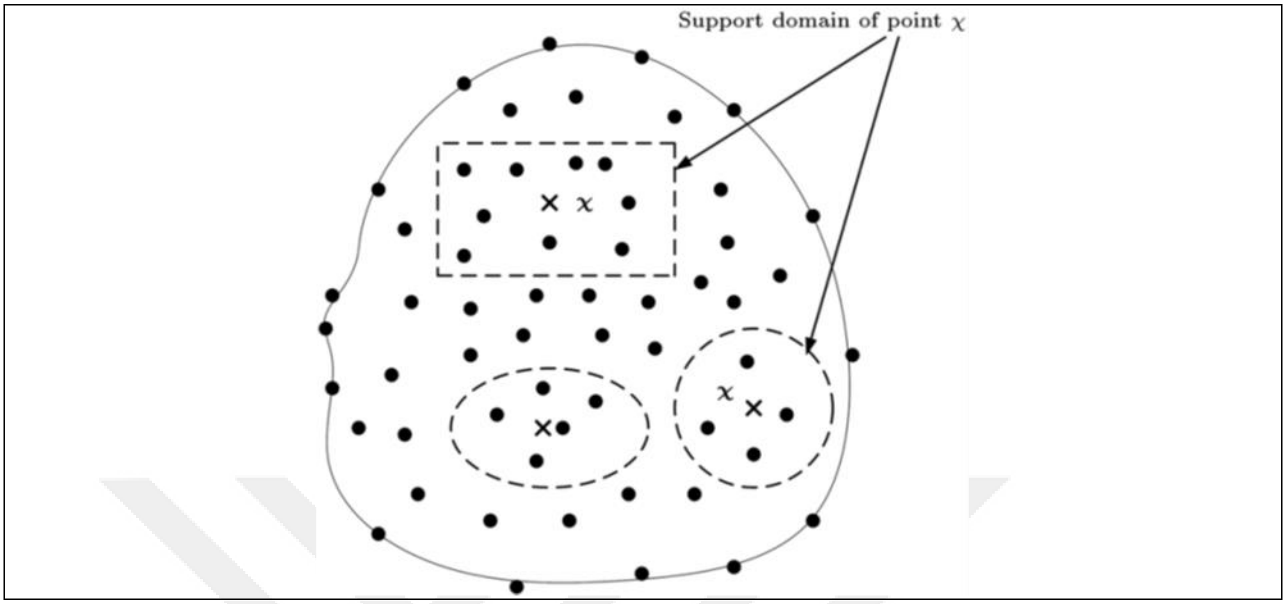

Figure 2. 4: Support Domains of Different Points[19]

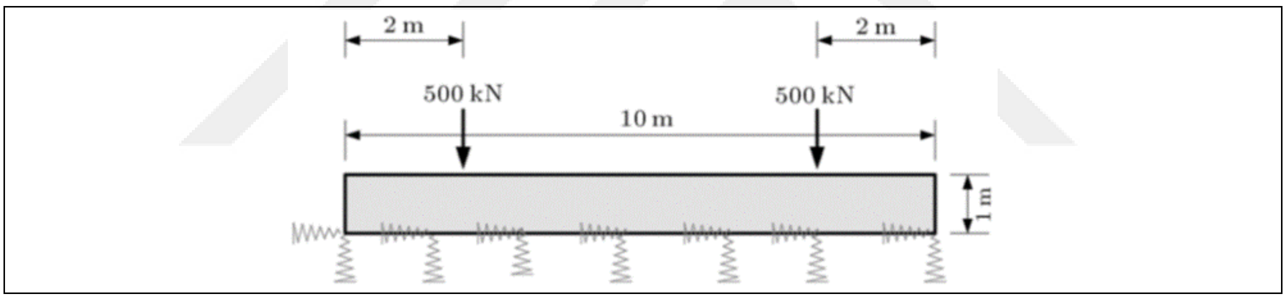

Figure 2. 5: Typical Problem of Beam on Two Parameter Elastic Foundation[19]

He came to the conclusion that there is no link between nodes, and that they may be readily added or removed. This property provides mesh-free approaches a lot of credit, especially in adaptive analysis. The connection element approach simulates the elastic base, and no nodes or elements in the classic sense are required. As a result, without any further post-processing alteration, the stresses throughout the foundation layer may be easily identified. Aside from all of these advantages, the findings' accuracy is adequate, using the same order of nodes, even better than finite element results.

B. Omolofe et al. [20]Moving force and mass models' fourth order partial differential equations with variable coefficients were solved analytically. Figure 2.6 shows a diffused beam. The dynamical system resonance phenomena is explored in detail for each of the essential boundary conditions.

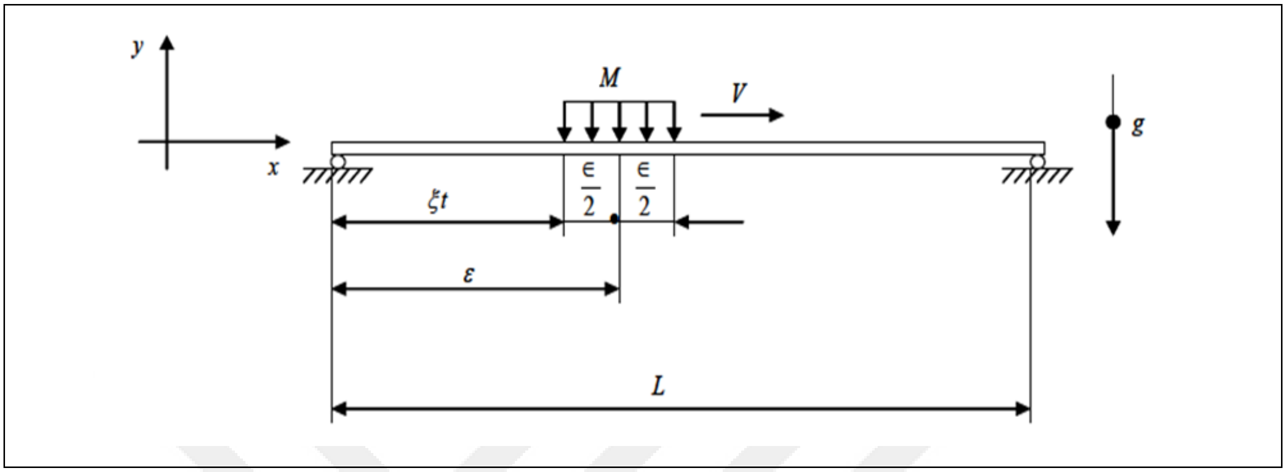

Figure 2. 6: Schematic Diagram of A Beam Under Partially Distributed Load[20]

The effects of uniform somewhat scattered stresses on a uniform Bernoulli-Euler beam were explored.

The results also reveal that in the case of a moving mass problem, larger values of the structural parameters K, N, and G are required than in the case of a moving force beam problem. The existence of structural components N, K, and G considerably improves the dynamic stability of a moving load on an elastic beam. For both moving distributed force and mass issues involving Bernoulli –Euler beams, this work has supplied incredibly useful information on the conditions under which the vibrating system may experience undesired resonance phenomena known as resonance.

Qijian Liu et al. [15] proposed an analytical solution for Euler-Bernoulli beams on elastic bi-dimensional foundations was discovered by assessing the beam-foundation system's horizontal and vertical displacements. The method uses a newly updated Vlasov model. Displacement function at ground surface, attenuation function along foundation depth, after variables are separated. So, how can you build governing equations and boundary conditions using variation? The differential operator breaks the connection between the governing equations and the boundary conditions. To complete the numerical implementation, iterative approaches are used.

Parametric study shows how applied stresses, physical and geometric features of the beam and foundations impact static reactions. Figure 2.7: Beams on elastic foundations[10].

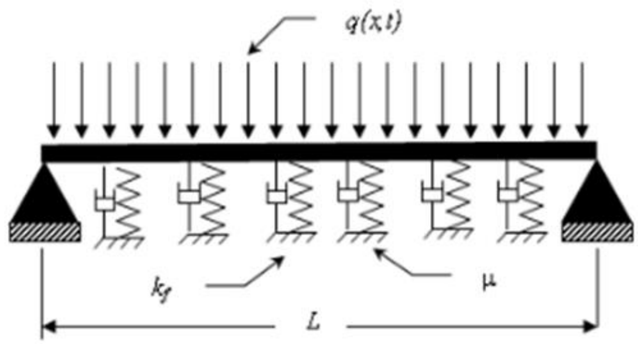

Figure 2. 7: Beam Resting on The Elastic Foundation[10]

There is a relationship between horizontal and vertical displacements in the beam-foundation system. Aspects of coupled beam static behavior are also significant.

Karel FRYDREK et al. [6] Numerical beam and frame solutions and 3D constructions on elastic foundations were investigated. In the first case, the solution is demonstrated using the ANSYS beam element BEAM54 and its stiffness matrix derivation. The second method uses a beam element and a contact element to obtain an elastic stiffness matrix derivative. Theoretical and practical approaches are compared. The response accuracy is influenced by the number of divisions in the beam element. External fixators, pressure distributions between mining supports and the foot-wall, rack-railway, and drop-in testing as a 3D body on an elastic foundation are just a few examples.

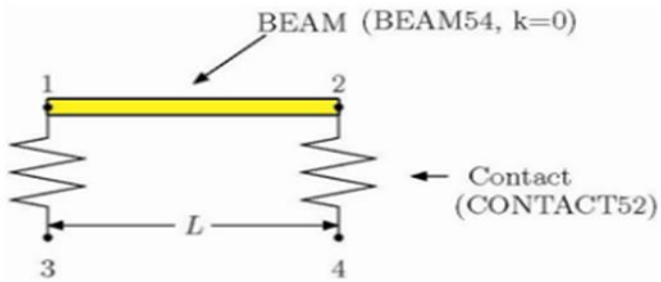

Figure 2. 8: Example of a Beam Resting on an Elastic Foundation. This beam is loaded by force (F), couple (M) and distributed loading (q)[6]

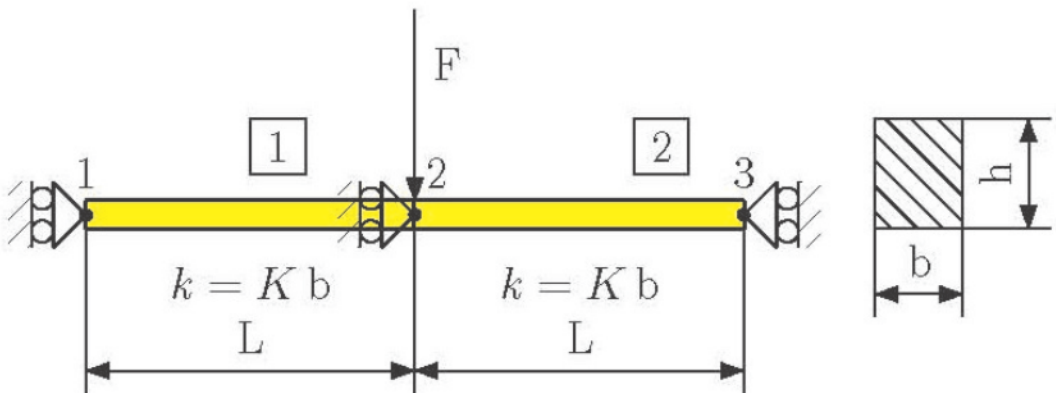

Figure 2. 9: FE Model[6]

General solutions for plane beam constructions on elastic (Winkler's) foundations were obtained, tested, and discussed using FEM applications (theory and practice) (two ways). The authors place a strong emphasis on the construction of FEM matrices.

Other personal examples (reports) include mining and biomechanical applications, dynamics, drop-in testers, and so on.

A.H. Sofiyeva et al.[21] These thin orthotropic circular cylindrical shells with geometric non-linearity of Karman type were studied analytically. Then, for laminated thin orthotropic circular cylindrical shells, Donnell type stability equations. A nonlinear time dependent differential equation is used to do this. The frequency is shown as a function of the amplitude of the shell displacement in this equation. Finally, non-linearity, non-homogeneity, layer number, and ordering affect frequency.

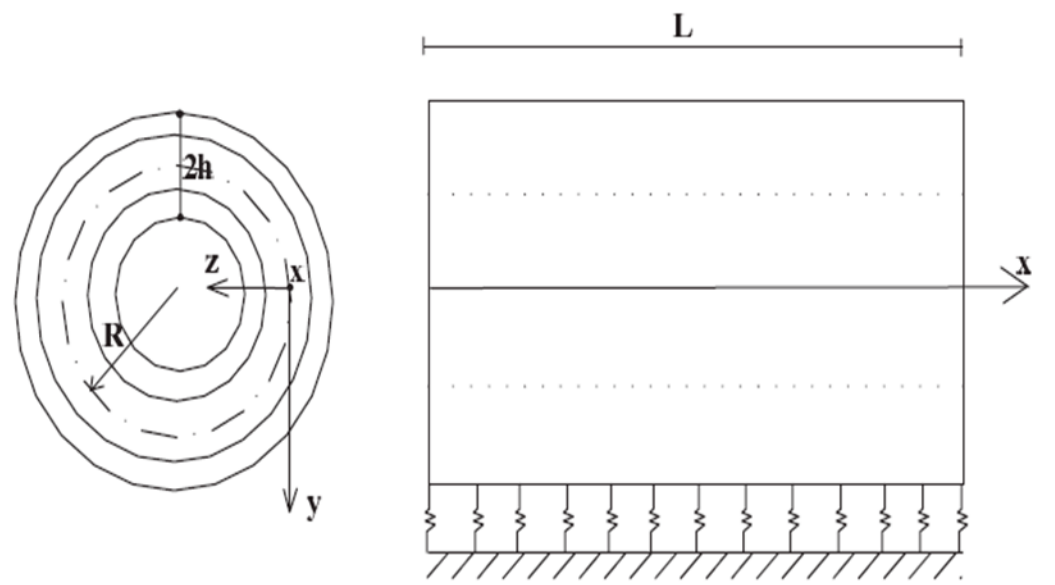

Figure 2. 10: Laminated Cylindrical Thin Shell on Elastic Foundation[21]

They determined that when the influence of the elastic basis is ignored, geometrical nonlinearity, non-homogeneity, and the number and ordering of layers have a significant impact on frequency values. The effects of the factors in question on frequency values lessen as the foundation modulus increases, and these variables have no effect on frequency values at higher foundation modulus values.

Natural frequency values increase as the ratio of shell thickness to radius (h1/R) increases. The findings of the research were then compared to those found in the literature, which proved to be correct[22].

K. L. Ravisankar et al.[23] are working to improve concrete's applicability and performance by addressing the aforementioned flaws. Shrinkage cracking is also reduced when fibers are added. Polypropylene was employed as the fiber. Polypropylene fiber, often known as polypropylene or PP, is a synthetic fiber made from 85% propylene and utilized in a wide range of applications. Polypropylene Fiber Reinforced Concrete is an emerging building material that may be characterized as a concrete with high mechanical strength, stiffness, and durability. It is employed in a variety of sectors.

Compressive strength tests were performed on cubes at 7 and 28 days after curing, and the cubes were cast with various proportions of mixed Polypropylene addition to cement weight, as shown in table 2.1.

Table 2. 1: Compressive Strength of Concrete[24]

Specimen No.	Proportional	7 days	28 days
1	Conventional	23.25	32.58
2	0.4%	16.62	29.18
3	0.6%	23.99	34.66
4	0.8%	25.62	37.62
5	1.0%	23.25	32.29

They observed that polypropylene fibers, owing to their flexibility and ability to bend to shape, reduce the quantity of plastic shrinkage fractures. The inclusion of 0.1 percent fibers by volume has been proven to reduce cracking by a factor of 5 to 10. The extent of fracture reduction is determined by the fiber content of the concrete. However, at this phase of the project, I'm looking at M30 concrete. According to the IS standard, each series consists of cubes, cylinders, and prisms. At the age of 28 days, a battery of tests was performed to determine compressive strength.

Ashish Kumar Yadav et al. [24] For various quantities of polypropylene fiber, such as 0 kg/m3, 3 kg/m3, 4 kg/m3, and 5 kg/m3, the mix design of grade M25 was tested to provide real examples. (For instance, 0 percent, 0.12%, 0.16 percent, and 0.2 percent.) To determine the compressive strength of each concrete grade, cube specimens were cast, cured, and tested at 7 and 28 days. To determine the split tensile strength and flexural strength of each concrete grade, a cylinder and prism were cast, cured, and tested for 28 days. In the behavior of a structural component (RCC beam) was also investigated with different polypropylene fiber proportions as part of the investigation.

The study examines the impact of polypropylene fiber in the development of mechanical characteristics in concrete. The specimens were cast as cubes (150mm x 150mm x 150mm), cylinders (15cm diameter and 30cm length), prisms (500cm x 100mm x 100mm), and structural component beams, as shown in Figure 2.11. (1.5m x 150mm x 200mm).

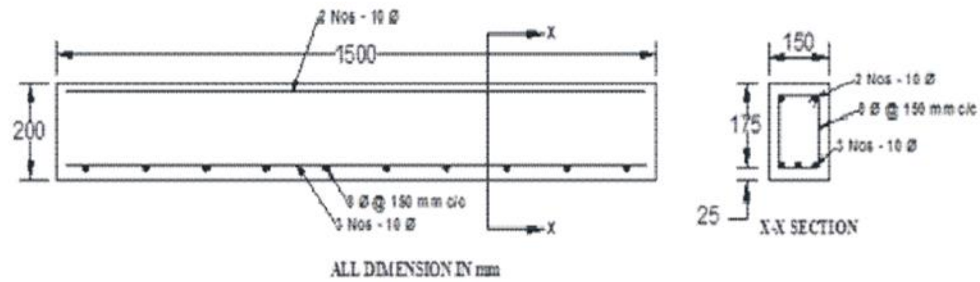

Figure 2. 11: The Specimens' Geometry and Reinforcement[24]

The beam specimens were bending tested in a servo control compression-cum-flexural testing equipment, as illustrated in figure 2.12.

Figure 2. 12: Experimental Setup[24]

The researchers determined that adding polypropylene fibers had no influence on compressive strength. The compressive strength of M25 grade concrete increases by 1% and 2% for 7 days and 28 days of maturity, respectively, when polypropylene fiber is added at a rate of 4 kg/m3. The compressive strength of polypropylene fibers decreases as the number of fibers increases.

The split tensile strength of M25 concrete increases by roughly 18% when polypropylene fiber is added at a rate of 5 kg/m3. Flexural strength rises by around 11% when 4 kg/m3 polypropylene fiber is added to M25 grade concrete, but subsequently declines when additional fiber is added.

Workability looks to be deteriorating with the addition of polypropylene fiber. The ultimate load bearing capacity of RCC beams increases by up to 12% when 5 kg/m3 polypropylene fiber is added to M25 concrete.

R. Zhang et al. [25]studied the influence of shear reinforcement amount on PP-ECC beam shear capacity. A 0.42 percent shear reinforcement ratio RC control beam. A total of five more PP-ECC beams were produced, with shear reinforcement ratios ranging from 0% to 0.40%. As a comparison, a second RC beam was made without shear reinforcement.
The uniaxial tensile technique was used to examine the tensile characteristics of PP-ECC. The plates used in uniaxial tensile testing had a cross sectional size of 7613 mm, as indicated in figure 2.13 (a) specimen dimensions (b) test setup). Dimensions and reinforcing details are also shown in figure 2.14.

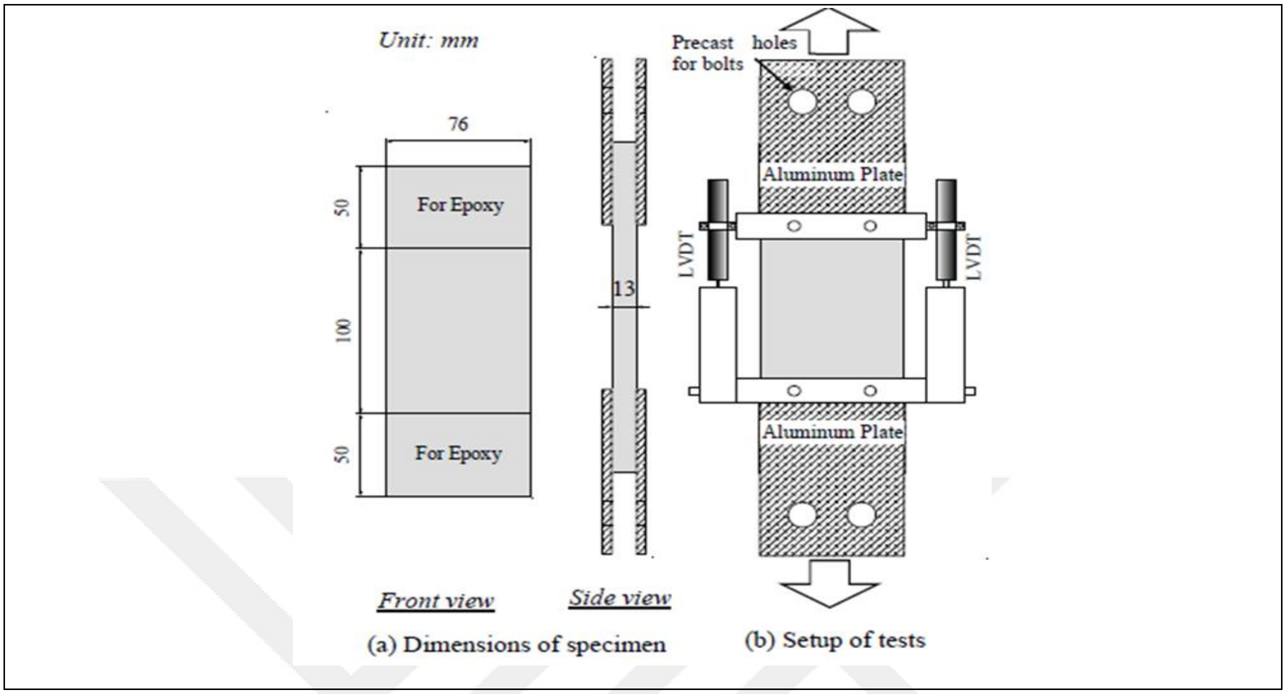

Figure 2. 13: (a) Dimensions of Specimen (b) SETUP of Tests[25]

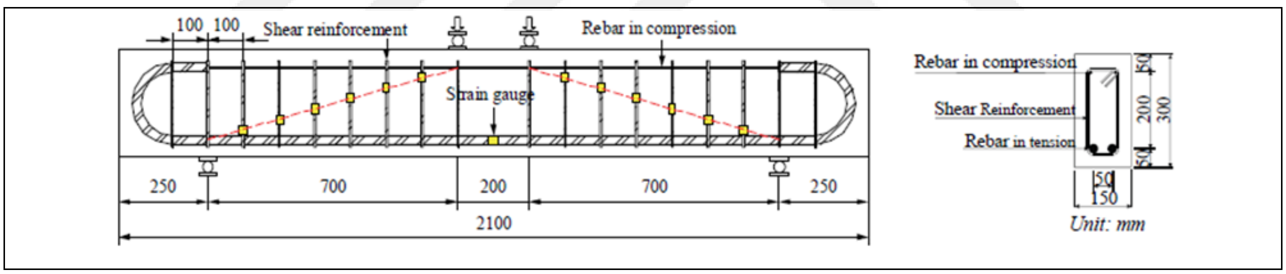

Figure 2. 14: Dimensions and Reinforcement Details[25]

They calculated that by replacing concrete with PP-ECC, the shear carrying capacity of the beam with shear reinforcements and without shear reinforcements increased 20.6 percent and 107.6 percent, respectively, due to the absence of coarse aggregates in PP-ECC, which affects its fiber bridging effect. The shear carrying capacity may be enhanced by switching from concrete to PP-ECC as the cement matrix, especially when the shear reinforcement ratio is low.

When comparing PP-ECC beams with greater shear reinforcement ratios at peak load to those with lower shear reinforcement ratios, the damage to the fiber bridging effect caused by sliding on the crucial fracture surfaces is more pronounced. This is one of the reasons why the shear carried by ECC in PP-ECC decreases when shear reinforcement ratio increases.

When the shear reinforcement ratio in a PP-ECC beam is increased, the angle of the critical fracture to the beam axis decreases, resulting in a reduction in the shear carried by fibers along the critical crack. With the rise in shear reinforcement ratio, this leads in a decrease in the shear borne by PP-ECC. Unlike in RC beams, where the shear carried by concrete remains nearly constant despite changing shear reinforcement ratios and the shear carried by shear reinforcement is proportional to the shear reinforcement ratio, the shear carried by ECC in PP-ECC beams decreases as the shear reinforcement ratio increases. The combined impact of reduced shear carried by fibers along the critical fracture and increased damage to fiber bridging generated by sliding along the critical crack surfaces results in a decrease in shear carried by fibers.

The existing JSCE code does not account for the fact that the shear carried by fibers in ECC reduces when the shear reinforcement ratio increases owing to sliding. This might lead to an overestimation of PP-ECC structural members' shear capability.

In a theoretical and practical work, Luay M. Al-Shather et al.[26] studied the shear behavior of RC I-beams employing polypropylene fiber and various volume fractions of plastic fiber as additive. In the present age, it has become increasingly vital to increase the sustainability of structural components by improving their mechanical performance by adding new materials such as plastic raw materials, notably I-beams used in long span constructions to become more ecologically friendly. In this study, which included seven specimens, just the amount of fiber volume fraction was changed.

As illustrated in figure 2.15, each specimen has the identical geometry: depth (h = 350 mm), flange width (bf = 160 mm), flange thickness (tf = 50 mm), web thickness (tw= 60 mm), and concrete cover (c = 15 mm).

The I-section Reinforced Concrete Beam's geometry and sectional dimensions are shown in Figure 2.15.

A half of the whole model was used for demonstration, taking advantage of the tested beam's symmetry. This method resulted in a considerable reduction in computing time. Figures 2.16 and 2.17 represent half of the entire model.

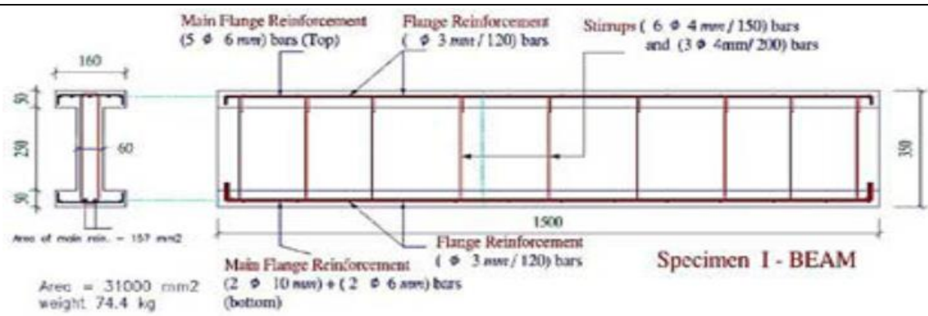

Figure 2. 15: Geometry and Sectional Dimensions of the I-section Reinforced Concrete Beam[26]

A half of the whole model was used for demonstration, taking advantage of the tested beam's symmetry. This method resulted in a considerable reduction in computing time. Figures 2.16 and 2.17 represent half of the whole model.

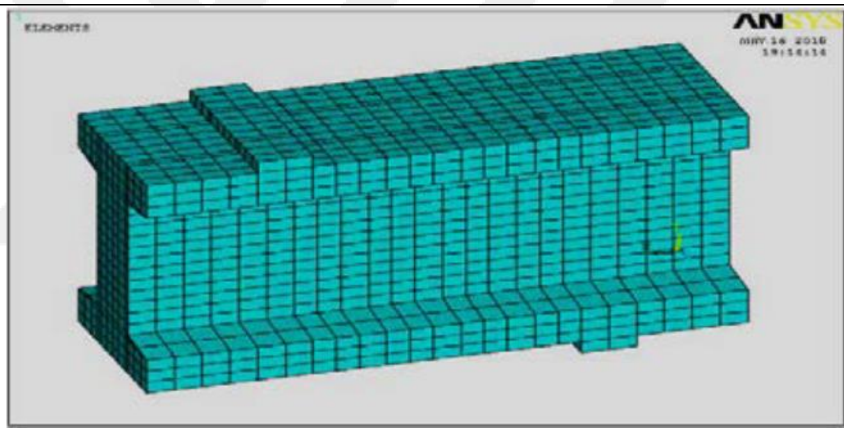

Figure 2. 16: Typical Half Symmetry Finite Element Model[26]

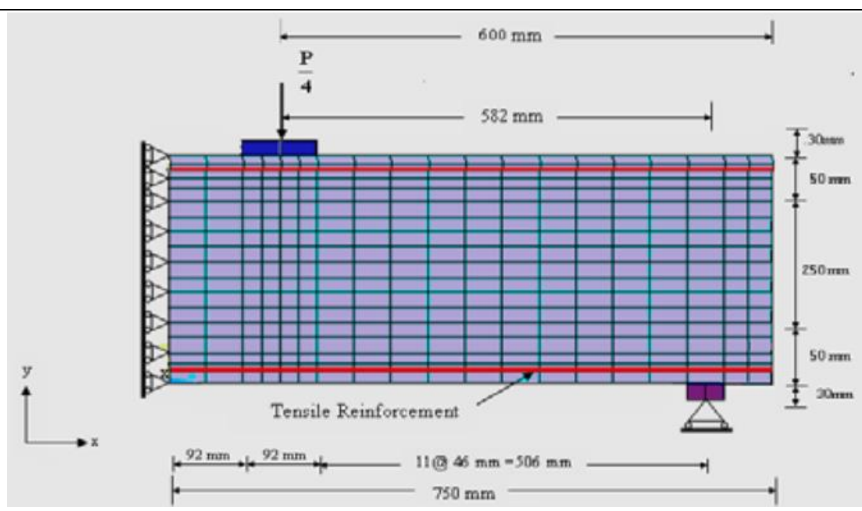

Figure 2. 17: Typical Half Symmetry Finite Element Model with Dimensions[26]

Due to the influence of fiber material (PPFRP) in the concrete mix, Concrete's compressive strength improved from 7.42 percent to 23.82 percent, while its splitting strength improved from 8.36 percent to 92.7 percent. The ultimate load of the tested beams varied from (4.4 percent to 35.27 percent) that of control IB-1 due to the presence of fiber material (PPFRP) in concrete.

PPFRP was found in the concrete mixture of the tested beams, according to the results of the beams test. The addition of fibers to fibred beams delayed and reduced crack spread, resulting in higher load bearing limits before the initial breaking and the development of early shear fractures at higher loads. An I – beam composed of PPFRC material has a stronger load – deflection behavior than a normal concrete I – beam (IB-1). The load-deflection curves are based on a finite element simulation that matches experimental curves well. In any case, The finite element models show a comparatively close response in the linear parts and a typically stiffer reaction in the nonlinear areas due to the fiber material balled inside the concrete mix and non-optimal fiber distribution in experimental models.

PPFRP was found in the concrete mixture of the tested beams, according to the results of the beams test. The addition of fibers to fibred beams delayed and reduced crack spread, resulting in higher load bearing limits before the initial breaking and the development of early shear fractures at higher loads. An I – beam composed of PPFRC material has a stronger load – deflection behavior than a normal concrete I – beam (IB-1). The load-deflection curves reflect a finite element simulation that is in good agreement with experimental curves.

When Fatih Altun et al, [27]evaluated the performance of reinforced concrete beams with and without fiber, and found that both were outstanding. The areas under the experimental load and displacement curves of beams were compared to determine whether they were strong or weak, and this was done to see if they were strong or weak.

As shown in figure 2.18 and figure 2.19, concrete simple beams are supported at both ends, and the weight is spread out over a distance of L/3, as shown in figure 2.19.

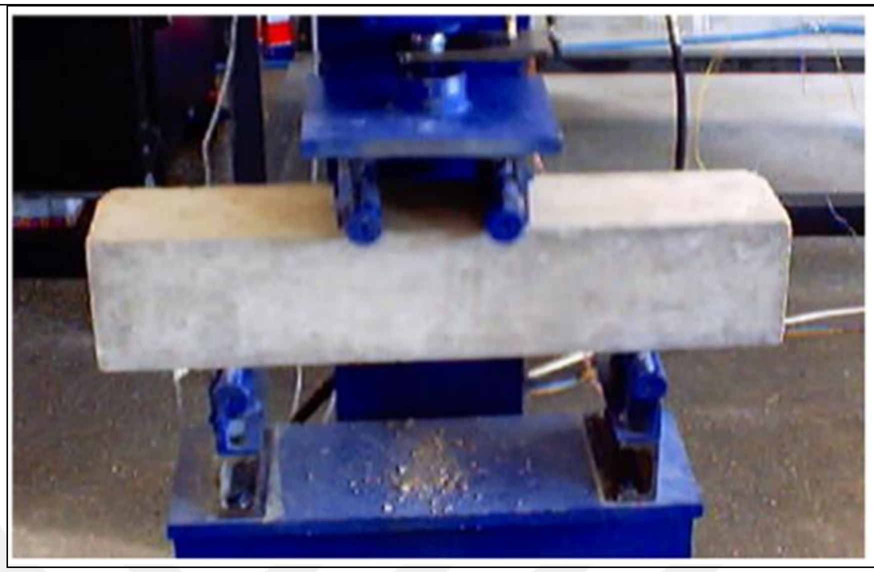

Figure 2. 18: Test Arrangement

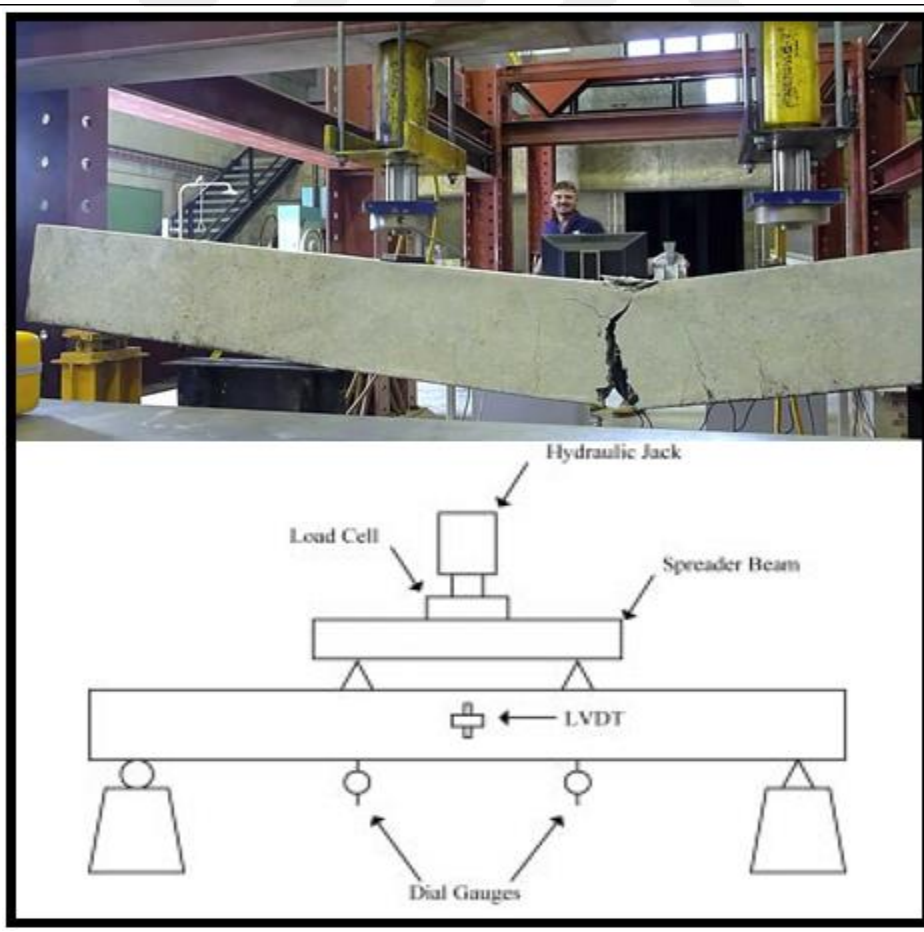

Figure 2. 19: Test Setup[27]

They compared the results. The comparison shows that reinforced concrete reference beams can absorb more energy than reinforced concrete beams reinforced with polypropylene fiber P-0.60 kg/m3, but have less ductility. Its ductility coefficient is 5.83 compared to 9912 kNmm for reinforced concrete reference beams, which is 4.71 for polypropylene fiber P-0.60 kg/m3. Reinforced concrete reference beams with polypropylene fiber P-0.60 kg/m3 have a 2% greater energy absorption capacity and a 23% higher ductility than reinforced concrete reference beams without polypropylene fiber. Reinforced concrete beams with polypropylene fiber P-0.60 kg/m3 are more ductile and perform better in seismic tests.

Musitefa Adem Yimer et al. [28]Examine the seismic behavior of SFRC beam-column junctions with varying axial loads. Figure 2.20 (a), (b), and (c) show nonlinear finite element analysis in ABAQUS/Standard using a damaged plasticity model (c).

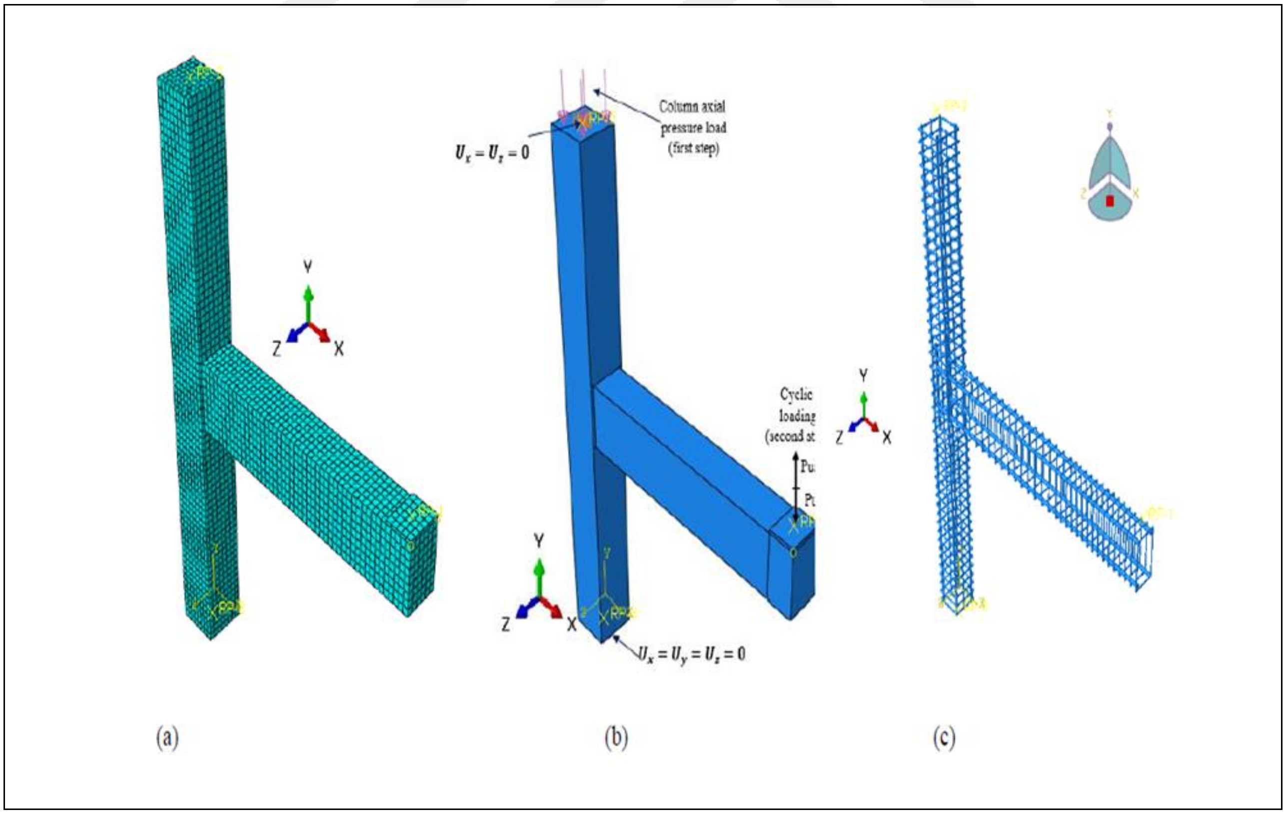

Figure 2. 20: Boundary Conditions, Meshing and Loading of the fee Model[28]

The finite element model is validated using experimental data from other researchers. Under reversed cyclic stress, six SFRC specimens with varied column axial load ratios and a 2% volume percentage of steel fiber were simulated, as illustrated in figure 2.21. Maximum load-carrying capacity, stiffness deterioration, energy dissipation, and failure mode are among the criteria examined.

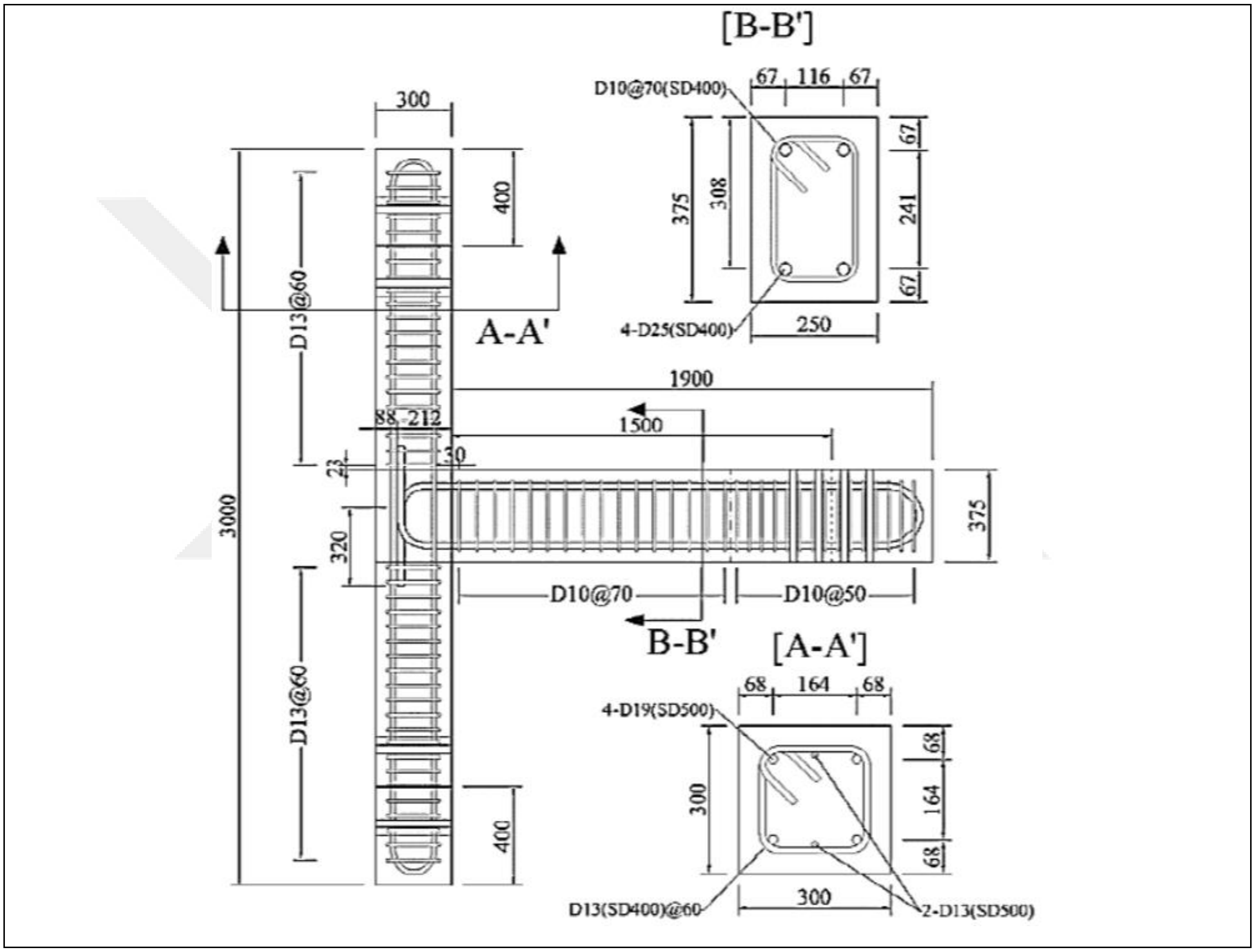

Figure 2. 21: Details of the Specimen[28]

The researchers determined that increasing axial stress had a significant impact on delaying the beginning of fractures and damage buildup. Furthermore, It is noted that when the axial load surpasses 50% of the column capacity, there are no fractures in the joint area, just flexural cracks at the beam-column interface.

The column axial load level might be increased from 5% to 30% of the column axial capacity to improve maximum load bearing capability of beam-column joints. When the axial load on the column is raised by more than 30%, the maximum load-carrying capacity of the joints does not change significantly from when there is no axial force. Increasing the axial load levels on columns improves the energy dissipation capacity of joints at the beginning of the loading process, but it has a little negative influence as the loading stages progress owing to axial failure and local concrete crushing.

The formation of cross diagonal fractures was inhibited when the column axial load level was increased, resulting in a minor improvement in joint stiffness. This is due to the axial load's restricting influence on joint shear. The cyclic stiffness dropped somewhat when the axial load exceeded 50% of the column capacity, due to degradation induced by local concrete crushing in the column. As a consequence of the findings, it appears that increasing column axial load enhances SFRC beam-column joint confinement; nevertheless, a threshold limit may be necessary.

3. METHODOLOGY

The (FEM) is a widely used approach in civil engineering and other technical fields for statistically assessing a broad variety of problems. This chapter outlines all of the project's methodologies for investigating the behavior of concrete beams. The mechanical characteristics of a concrete beam were investigated using a model in this study. Various loads will be applied to the concrete beam. The concrete beam foundation will be affected by these loads. This research is focused on the impact of an elastic basis on the stability and vibration of a concrete beam[29]. The application of various numerical approaches and a variety of computational algorithms to solve and analyze structural and materials challenges. In order to analyze the impacts of several critical characteristics, such as beam thickness and material composite system, the analysis includes them. A parametric analysis was conducted to look at the factors that can have the most impact on the mechanical behaviors of the model, such as changing the loading types. The goal of this project is to develop a numerical model that can predict the properties of concrete beam displacements and internal forces in elastic foundations as a result of the applied load. The ANSYS software tool was used to simulate the interaction of structural elements with various effective parameters and beginning circumstances. The approach used in this study will test the model by discretizing the partial differential equations into a limited set of control volumes known as meshes and cells[30]. The solver will then prepare ANSYS, which is a huge general-purpose finite element computer software with more than 180 different types. It has the ability to do both static and dynamic analysis. For more than two decades, it has been the most popular finite element analysis program. It is a very powerful and amazing technical tool that can be applied to a wide range of issues. The numerical study of the beam structure is carried out using a thorough FEM model created with the aid of the ANSYS Finite Element program's algorithms[31]. The coinciding nodes and elements are limited to be connected in the direction normal to the interface in order to meet the continuity criteria between the fluid and shell media at the cylindrical boundary, but relative motions are permitted in the tangential directions. The 3-D model is used to replicate the braces' uniaxial "tension alone" behavior.

3.1 BASIC STEPS IN FINITE ELEMENT METHOD

The following are the fundamental stages in every finite analysis[32]:

A. Preprocessing Phase

1. Subdivide the problem into nodes and elements and discretize the remedial domain into finite elements.
2. Assume a form function to reflect an element's physical behavior; that is, an approximate continuous function to provide an element's solution.
3. Produce an element's equations.
4. Assemble stiffness the elements to present the entire problem and construct the global stiffness matrix.
5. Apply the boundary, initial, and load carrying capacity.

A collection of linear or nonlinear algebraic equations is solved at the same time to get nodal results, such as temperature or displacement values at various sites in a heat transfer issue, Any other pertinent data, such as stresses and strains, that the nodes or elements may get.

B. Solution Phase:

To get nodal outcomes, such as displacement or temperature values at different nodes, concurrently solve a collection of linear or nonlinear algebraic problems.

C. Postprocessing Phase:

Obtain additional important data, such as major stress levels, heat fluxes, etc.

3.2 MATERIAL IDEALIZATION

The finite element approach is commonly used to discover approximate solutions for structures with intricate geometries, changeable materials, and loading arrangements in the subject of solid mechanics. According to the ANSYS computer software, this chapter will cover all of the aspects idealization and key choices (KEYOPT) employed in the current study[33].

3.2.1 Finite Element Model of Beam

In the ANSYS program, a four nodal isoperimetric clam element (SHELL63) was used to simulate a cylindrical storage beam, which incorporates both bending and membrane capabilities, as shown in Figure (3.1). In-plan and standard loads are both allowed. At each node, the element has six degrees of freedom: x, y, and z translations, as well as rotations around the x, y, and z axes. Large deflection capabilities and stress stiffening are incorporated[34].

3.2.2 Element Key Options Supported by ANSYS

The SHELL63 element makes modeling linear, curved, and reasonably thin shell structures simple. Elasticity, stress stiffening, and a significant deflection are all characteristics of the element. As shown by the beam d values in Figure 3.1 and table, Pressures can be used to put surface loads on the faces of an element.3.1[35].

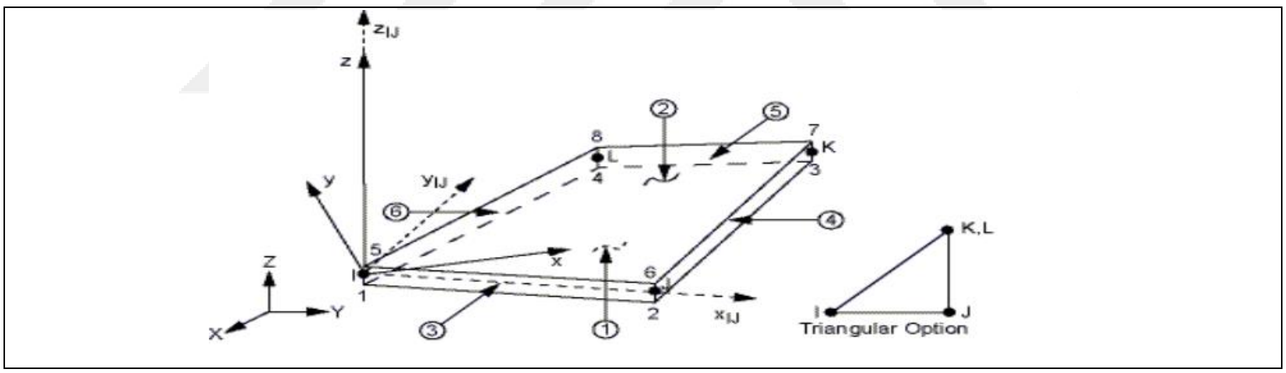

Figure 3. 1: SHELL63 Element Geometry (ANSYS 2016)

3.3 FREE VIBRATION RESPONSE

When a structure is perturbed from its static equilibrium state and then allowed to oscillate spontaneously in the absence of external dynamic stimulation or support motion, it is said to be undergoing free vibration. The initial stage in determining the free vibration response of any structural system, such as natural frequencies and mode shapes, is crucial for estimating the seismic reaction of liquid storage beams. The response of any system may be determined by examining the system's governing equation of motion. This may be calculated using the following equation[36][37]:

This can be obtained from this Eq:

$$[M]\{\ddot{U}\} + [K]\{U\} = \{0\} \qquad (3.1)$$

Where [M] and [K] are the mass and stiffness matrices of the system, respectively; and {U} is displacement vector.

Therefore, the natural frequencies (ω) and the mode shapes $\{\phi\}$ of any system governed by Eq. (3.1) are solutions of the eigenvalue problem represented by:

$$\big[[\mathrm{K}] - \omega^2[\mathrm{M}]\big]\{\phi\} = \{0\} \qquad (3.2)$$

For non-trivial solution of Eq. (3.2),

$$\big[[\mathrm{K}] - \omega^2[\mathrm{M}]\big] = 0 \qquad (3.3)$$

The frequency equation of the system is Equation (5-3). For a system with m degrees of freedom, expanding the determinant yields an algebraic equation on the mth degree in the frequency parameter 2. The m roots of this equation denote the frequencies of the m possible modes of vibration in the system. The m roots of this equation $(\omega_1^2, \omega_2^2, \omega_3^2, \ldots \ldots \ldots \ldots, \omega_m^2)$ represent the frequencies of m modes of vibration which are possible in the system.

The Jacobi approach is a good choice if all m eigenvalues are required and m is reasonably small (approximately m 200), hence Eq. (3.3) is solved numerically by the Jacobi method presented by (Chandrupatla, in 1997) for all examples in all cases considered in the present study.

3.4 CONCRETE BEAM ELEMENTS

The ANSYS program was first utilized to check the formulation of the shell stiffness and mass of matrices of a beam by computing the natural frequencies and mode Shape when choosing the Model Analysis for two cases of boundary conditions[38]:

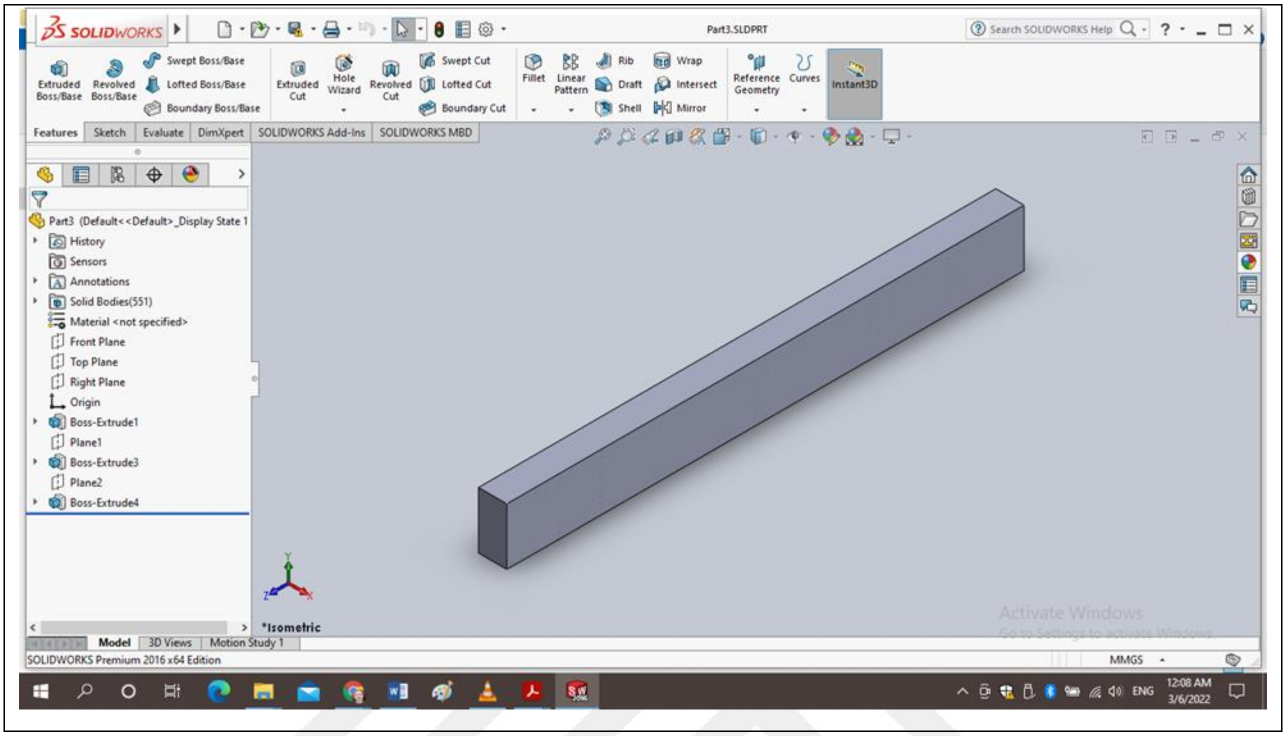

Figure 3. 2: Beam Element

3.5 MODEL EQUATIONS

This approach is used in ANSYS Program Call for this Analysis (Modal analysis) to find a structure's inherent frequencies and mode shapes. Modal analysis is the most fundamental kind of dynamic analysis since it determines how a structure responds to any type of dynamic stress. Always do a modal analysis prior to conducting any other kind of dynamic analysis [39][40].

General equation of motion is:

$$[M]\{\ddot{u}\} + [C]\{\dot{u}\} + [K]\{u\} = \{F_{(t)}\} \quad (3.4)$$

Assume free vibrations and ignore damping, you can be equation

$$[M]\{\ddot{u}\} + [K]\{u\} = \{0\} \quad (3.5)$$

Assume harmonic motion (i.e. $u = U\sin(\omega t)$)

$$([K] - \omega^2[M])\{u\} = \{0\} \quad (3.6)$$

a) The eigenvalues of this equation are wi2, where I range from 1 to the number of degrees of freedom. The eigenvectors ui correspond to the corresponding vectors.
b) The natural circular frequencies (radians/sec) of the structure are I the square roots of the eigenvalues. (fi = wi/2π) (cycles/sec) is then used to derive natural frequencies fi. It's the natural frequencies fi that the user enters and ANSYS outputs.
c) The eigenvectors {u}i denote the mode forms, or the shape that the structure takes while vibrating at a finite frequency fi.

The transformation of Eq. (3.5) to

$$[M]\{\ddot{\mathrm{U}}\} + [C]\{\ddot{U}\} + [K]\{U\} = -[M]\{R\}\ddot{U}_g$$

The normal coordinates by using the orthogonality property of the normal modes, gives a set of J uncoupled modal equations of the form:

$$M_j\ddot{Y}_j + C_j\dot{Y}_j + K_jY_j = P_j(t) \tag{3.7}$$

In which Y_j is the amplitude associated with mode J, P_j is the generalized force resulting from the earthquake excitation, and is given by:

$$P_j(t) = \{\phi\}_j^T P_{eff}(t) = -\{\phi\}_j^T[M]\{R\}\ddot{U}_g(t) \tag{3.8}$$

And M_j , C_j and K_j are the generalized properties, given as:

$$M_j = \{\phi\}_j^T[M]\{\phi\}_j \text{ , } C_j = [\phi]_j^T[C]\{\phi\}_j \text{ and } K_j = \{\phi\}_j^T[K]\{\phi\}_j \tag{3.9}$$

The mass and stiffness matrices, [M] and [K], are calculated using the techniques described in Chapter 3, whereas the damping matrix, [c], is written as:

$$[\mathrm{C}] = [\mathrm{M}]\left(\sum_{j=1}^{J}\frac{2\zeta_j\omega_j}{M_j}\{\phi\}_j\{\phi\}_j^T\right)[\mathrm{M}] \tag{3.10}$$

In which ω_j, ζ_j are the natural frequency and damping factor (which is assumed to be the same for all modes of vibration), respectively.

For an elastic system, the equation of motion, Eq. (3.11), may be solved numerically by different techniques. In the present analysis, the direct step–by-step integration based on Newmark's method is used to solve Eq. (3.11).

Many scholars created a family of time-stepping systems based on the equation below:

$$\dot{U}_{t+\Delta t} = \dot{U}_t + \left[(1-\gamma)\ddot{U}_t + \gamma\ddot{U}_{t+\Delta t}\right]\Delta t \qquad (3.11)$$

$$U_{t+\Delta t} = U_t + \dot{U}_{t+\Delta t} + [(0.5-\beta)\ddot{U}_t + \beta\,\ddot{U}_{t+\Delta t}](\Delta t)^2 \qquad (3.12)$$

The parameters β and γ specify the change of acceleration across a time step and govern the method's stability and accuracy. Typical selection for γ is $\frac{1}{2}$ and $\frac{1}{6} \le \beta \le \frac{1}{4}$ is satisfactory from all points of view, including that of accuracy. The parameters and are used to assess the method's stability and accuracy by specifying the variation of acceleration across time steps. The most common option for is and is acceptable in every way, including accuracy. Together with the equilibrium equation (3.11), they allow us to compute and at time t+t from the known, and at time t from the unknown. Iteration is required to finish these calculations since the unknown is on the right side of Eq. (3.11).

3.6 MODELLING THE CONCRETE BEAM

This section aims to produce a numerical model capable to predict the concrete beam characteristics in simulated model in order to investigate the beam behaviour. The calculations required simulating the interaction of structural with different effective parameters, and initial conditions are done by the ANSYS software program. The partial differential equations are solved numerically to render the solution field based on structural analysis. The procedures utilized throughout this project as shown in the flow chart in Figure 3.3.

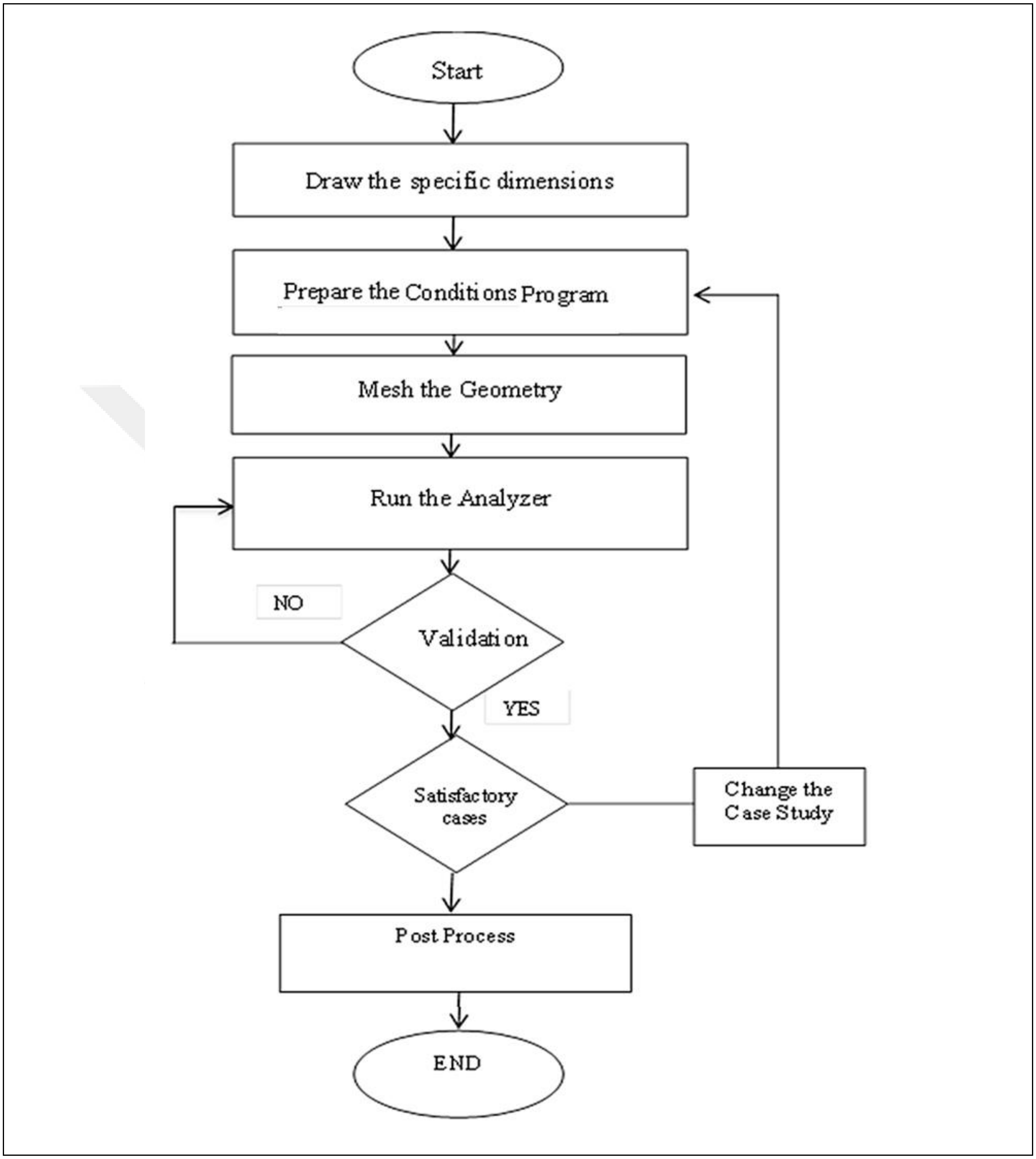

Figure 3. 3: Flowchart of the Project

3.7 MODELLING IMPLEMENTATION

Modeling is a visual representation of the construction and functioning of a system. A model is a representation of a system that is similar to but not identical to the system being represented. One of the objectives of a model is to enable the analyst to predict the effect of system changes. On one side, a model should closely depict the actual system, with the bulk of its main properties included. On the other hand, it shouldn't be so sophisticated that it's impossible to grasp and experiment with. Figure 3.4 depicts the general modeling solution procedures. The ANSYS modeling process may be broken down into a few key steps:

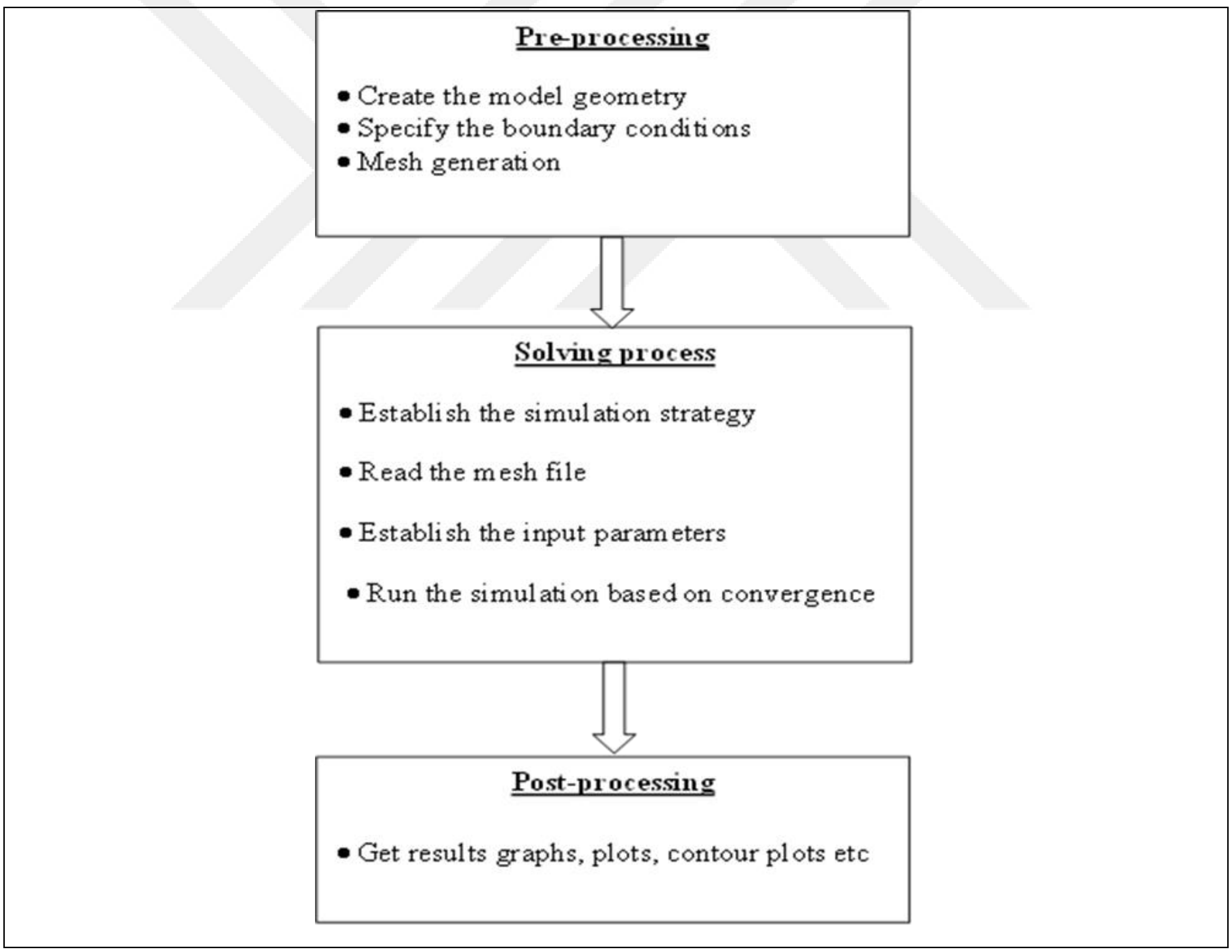

Figure 3. 4: The ANSYS Modelling Sequence

A good model is a careful balance of realism and simplicity. ANSYS is a commercial software program that may be used to address structural problems. ANSYS structural analysis software is capable of modeling every structural component of a product, from basic linear static analysis to advanced nonlinear transient events with dynamic effects and complicated behaviors.

3.8 PRE-PROCESS IN THE ANSYS ENVIRONMENT

The procedure of identifying the parameters of the chosen material model from the ANSYS database was carried out in the ANSYS environment using numerical calculations on the model database. The cornerstone for the optimization or assessment procedure is the initial data of material properties. The amount of money needed for preliminary research is determined by the study's limits and objectives. The primary duty of the initial study is to ensure that all studies cited in establishing limits and goals are from the same technical data set. Figure 3.5 shows the ANSYS engineering data for an actual model implementation.

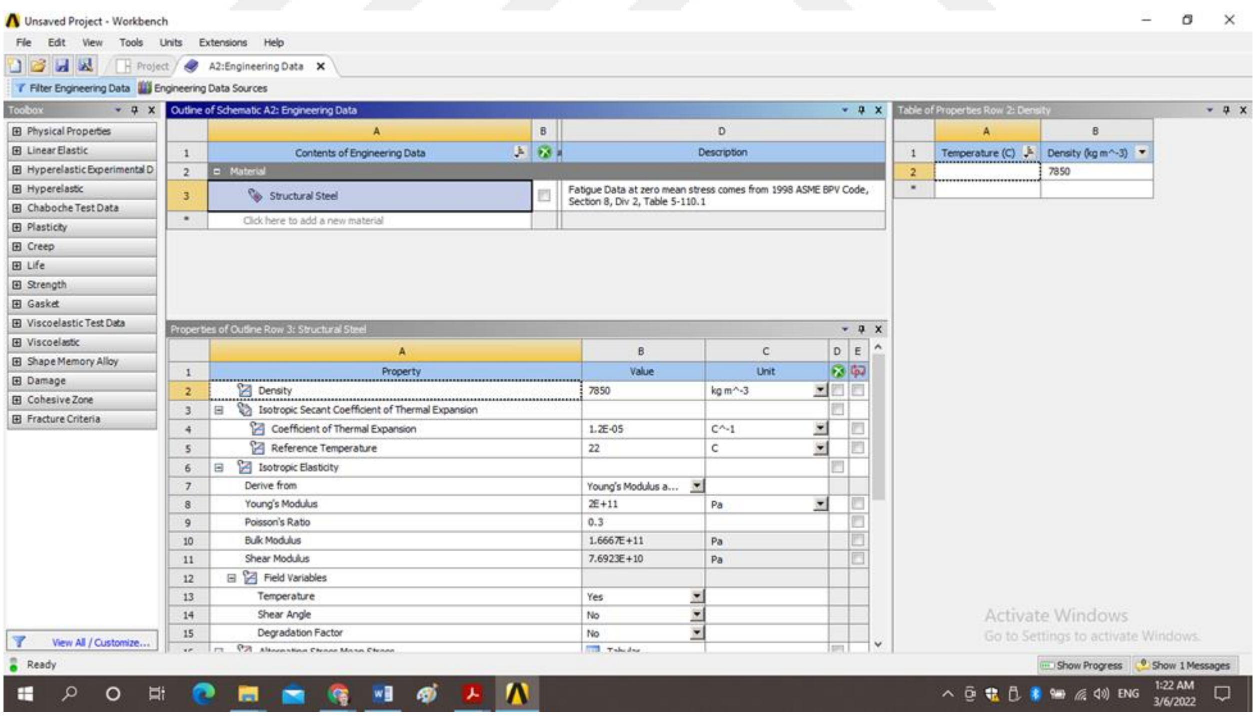

Figure 3. 5: Engineering Data of Elements Type Definition

Step 1**:** specify static structural

Organizations all across the globe rely on ANSYS structural analysis software to quickly address difficult structural engineering challenges. ANSYS' finite element analysis (FEA) software allows you to model every structural feature of a product. ANSYS vibration analysis was used to investigate advanced transient nonlinear phenomena with dynamic effects and complex behavior. The ANSYS Workbench easy workflow is provided, as is a broad variety of material models, element library quality, solver speed, robustness, and accuracy. ANSYS simulations may be made much faster by using multiple core PCs and High Performance Computing (HPC). Smooth geometry input, parametric research, and optimization are all possible thanks to bidirectional interfaces with all major CAD systems. Meshing single component and assembly models is straightforward to set up and prepare thanks to automatic contact detection. Other features, such as built-in simulation wizards and factor-of-safety prediction, allow even inexperienced users to quickly get accurate and reliable simulation results. ANSYS CFD software can conduct (FSI) and other multiphysics simulations when used in conjunction with ANSYS Fluid Mechanics or Electromagnetics solvers.

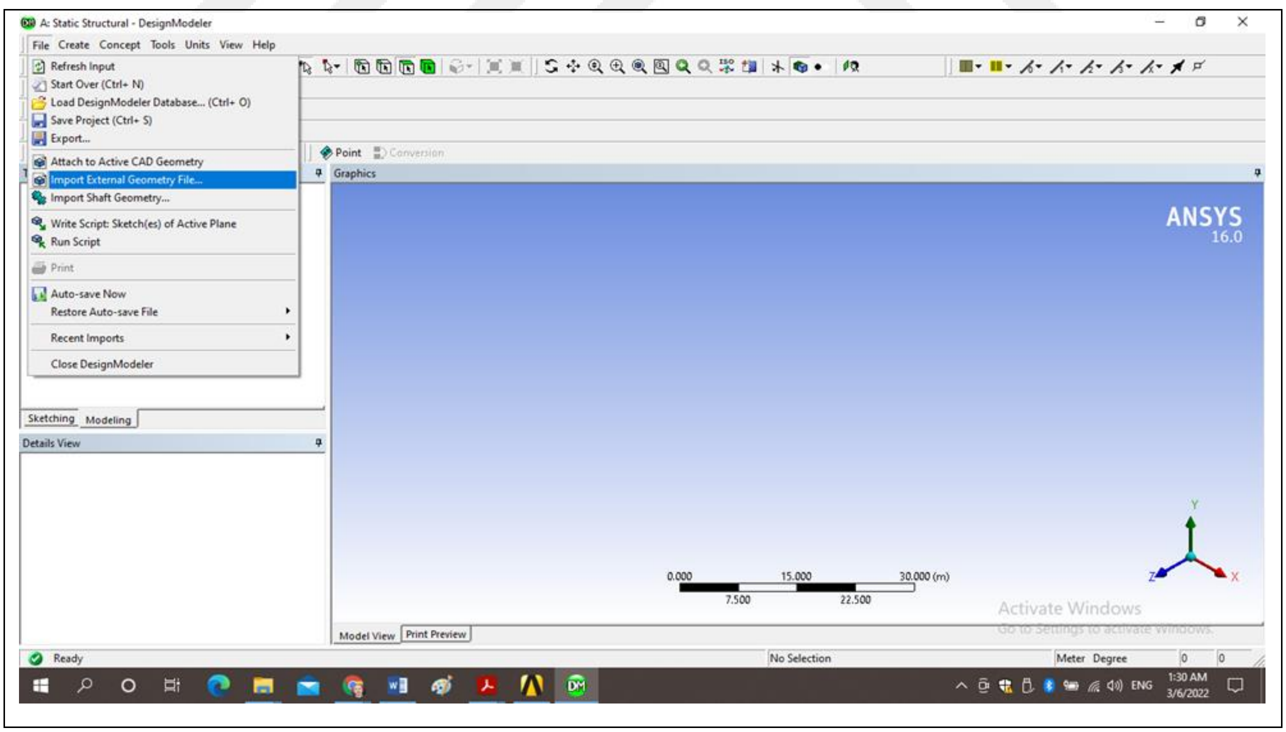

Figure 3. 6: Import Geometry

Step 2: Used Material Properties:

a) In today's technology civilization, construction materials are in high demand, also known as building materials. A wide range of building materials are used in diverse construction projects.
b) The cement: the qualities of regular strength cement. Concrete made with Portland cement:
c) Steel fiber: the typical properties of normal strength steel fiber materials

Table 3. 1: Cement Properties

parameter	value
Density - ρ:	2240 - 2400 kg/m3 (140 - 150 lb/ft3)
Compressive strength:	20 - 40 MPa (3000 - 6000 psi)
Flexural strength:	3 - 5 MPa (400 - 700 psi)
Tensile strength - σ:	2 - 5 MPa (300 - 700 psi)
Modulus of elasticity - E:	14 - 41 GPa (2 - 6 x 106 psi)
Permeability:	1 x 10-10 cm/sec
Coefficient of thermal expansion - β:	10-5 oC-1 (5.5 x 10-6 oF-1)
Drying shrinkage:	4 - 8 x 10-4
Drying shrinkage of reinforced concrete:	2 - 3 x 10-4
Poisson's ratio:	0.20 - 0.21
Shear strength - τ:	6 - 17 MPa
Specific heat - c:	0.75 kJ/kg K (0.18 Btu/lbm oF

Table 3. 2 : Steel Fiber Properties

parameter	Steel	
	S355	Wire
Density ρ (kg/m3)	7850	7850
Tensile Strength (GPa)	0.5	1.77
Elastic Modulus E (GPa)	210	210
Breaking Length σu/(ρg)(km)	6	23

d) Steel bars of steel reinforcement with 5.3 mm in diameter. the typical properties of normal steel bar materials

Table 3. 3: Steel Bars of Steel Reinforcement Properties

	Bar samples		
parameters	EC	ASTM A706	BS4449
Yield strength S, N/mm2	460.14	415	460
Ultimate tensile strength, N/mm2	597.21	580	600
Elongation, %	9.02	10	12
Reduction in area, %	22.15		

According to earlier researches and studies fibers are more active with a mixture with total mix percentage as shown in the Table 3.4.

Table 3. 4: Mix Design

Mix code	V_f %	Cement (kg)	Sand (kg)	Gravel (kg)	Steel fiber (kg)
1	0	10.5	26.5	17	0.0
2	0.75	10.5	26.5	17	1.3
3	1	10.5	26.5	17	1.75
4	1.25	10.5	26.5	17	2.2

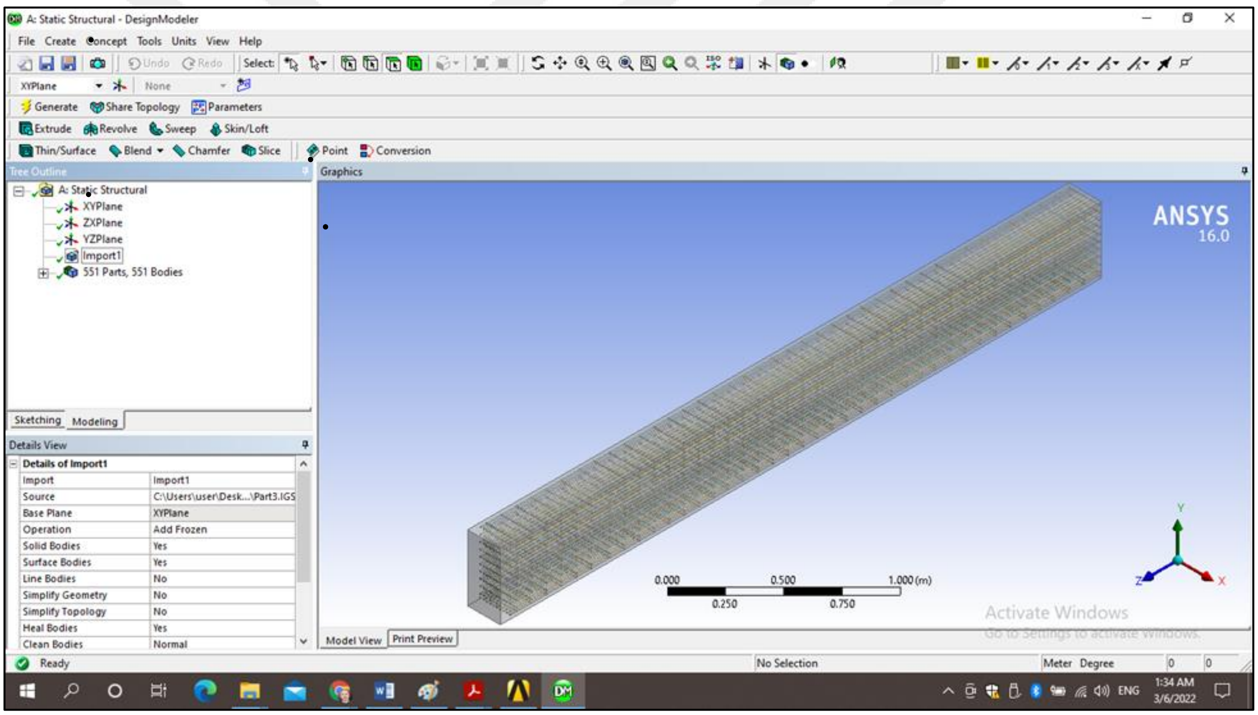

Figure 3. 7: Structural Reinforcing

In a structural reinforcing analysis, use REINF264 to add additional reinforcing to common 3-D link, beam, shell, and solid components (referred to as the base elements). The element may be used to simulate reinforcing strands of any orientation. Each fiber is represented as a single spar with just uniaxial stiffness or conductivity. Multiple reinforcing fibers can be specified in a single REINF264 element. The nodal placements, degrees of freedom, and connectivity of the REINF264 element are identical to those of the base element.

Step 3**:** meshing process

The geometry must then be meshed. It is necessary to utilize the ANSYS Meshing program to produce a computational mesh for the structural analysis throughout the slab volume. Setting element attributes and Mesh controls are required steps in the technique for creating a mesh of nodes and elements. A great range of mesh controls are available in ANSYS. The ANSYS Mesh Tool (Main Menu> Preprocessor> Meshing> Mesh Tool) provides a quick and easy way to access several of the most often used mesh settings and meshing processes. The Mesh Tool is an interactive "tool box" that you may use from the moment you start the operation until you shut it or depart PREP7. Although all of the Mesh Tool's functions are also accessible via conventional ANSYS commands and menus, the Mesh Tool provides a convenient shortcut. The Mesh Tool comes with a slew of options, including:

a) Managing the Smart Sizing levels.
b) Controlling the size of elements.
c) Defining the form of the element.
d) Choosing a meshing type (free or mapped).
e) Meshing solid model entities.
f) Clearing meshes.
g) Refining meshes.

There are two types of 3-D mesh elements: triangular and quadrilateral. When a triangle element is used, an unstructured mesh is created, however when a quadrilateral element is used, a structured mesh is created. When building a mesh, you may choose the element count (number of elements) or the element size. We can change the size of mesh-element edges for geometric edges, meshed faces, and volumes using the size functions. The case study should be discretized, according to the results of the meshing. Because it provides the finite element analysis, it is the most significant portion of an analysis and can decide the efficiency and efficacy of an analysis. As a result, meshing complicated models takes a long time. Figure 3.8 depicts the mesh output in our example study. It's worth noting that the boundary layer has a variety of discretizations, allowing us to examine the boundary layer in more depth and obtain more accurate findings. The amount of difficulty experienced in meshing the geometry is measured by meshing complexity. Mesh creation is recognized to be challenging due to a variety of factors such as near-tangencies, topological layout, and so on. The conversion of these issues into a measure that quantifies them is called meshing complexity.

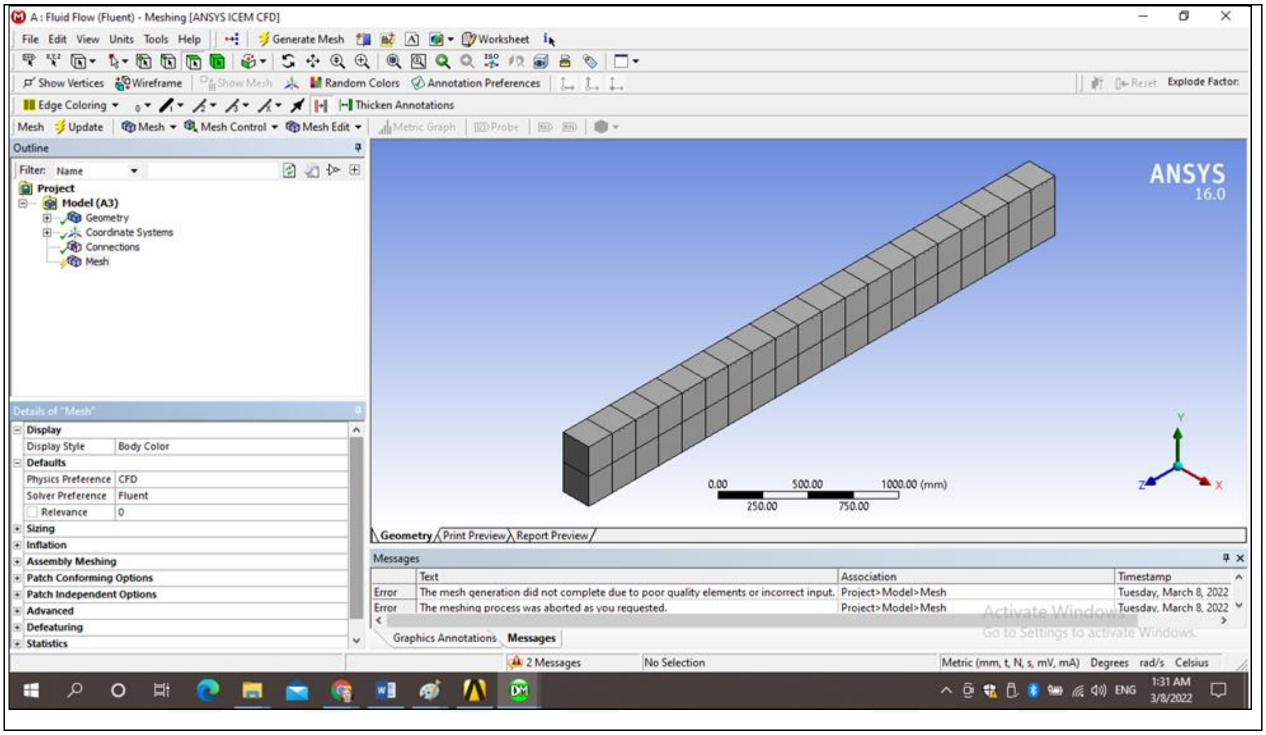

Figure 3. 8: Mesh File Configuration (1)

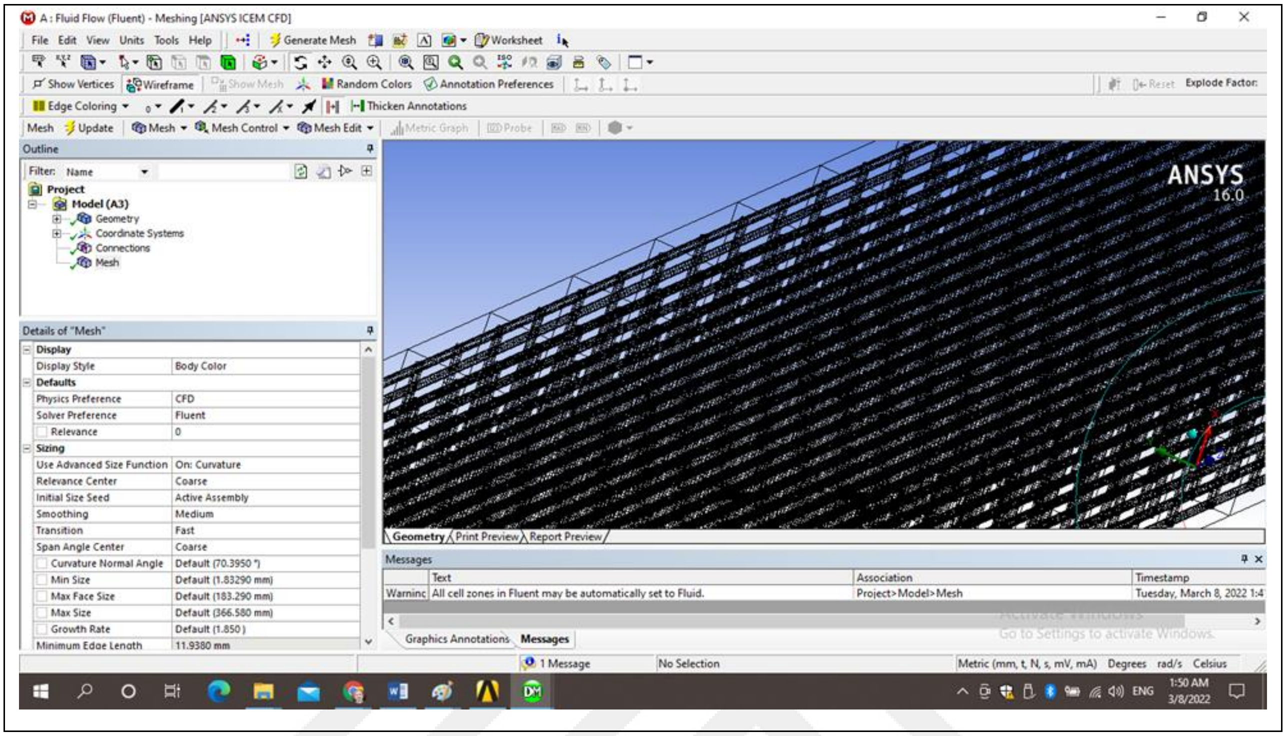

Figure 3. 9: Mesh File Configuration (2)

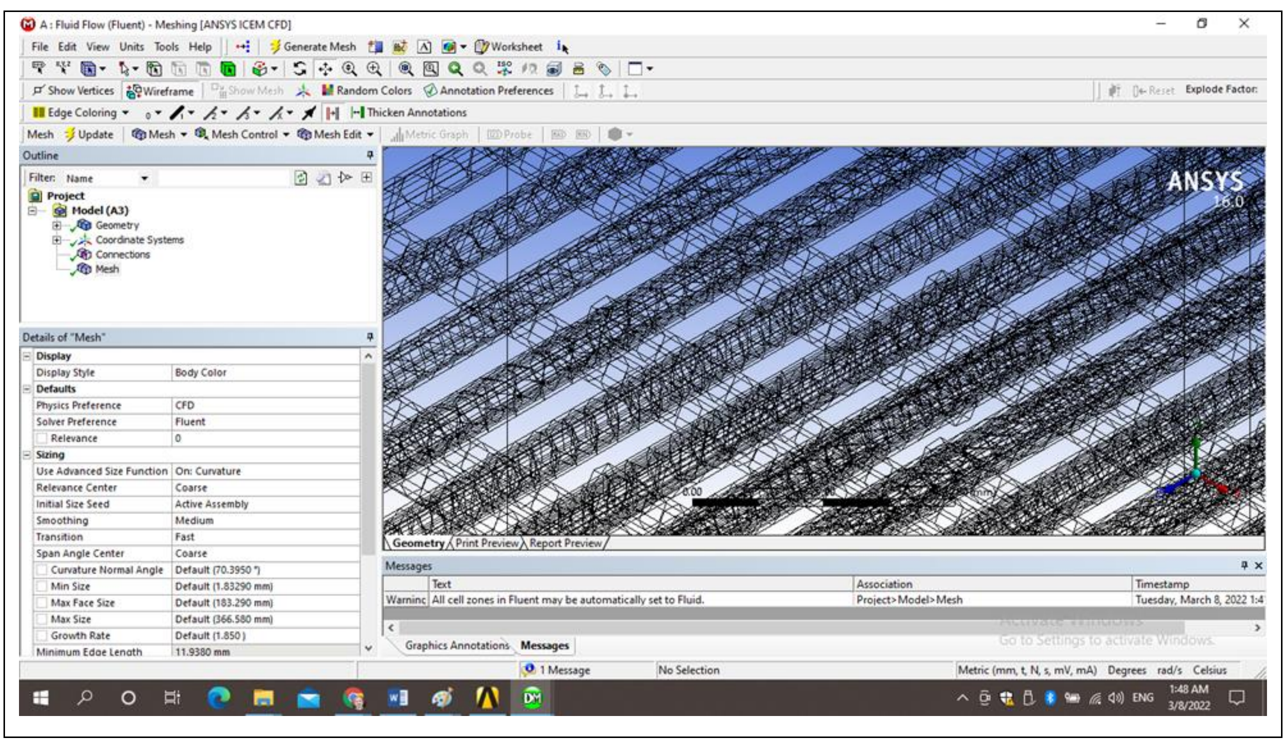

Figure 3. 10: Mesh File Configuration (3)

Many geometries, for example, have exceedingly mathematically complicated curves and surfaces yet been easily mesh able. Similarly, utilizing linear curves and flat surfaces, one might easily create a model that is practically hard to mesh. In this case, the metric may be used to identify invalid as well as potentially low-quality parts, which could result in a bigger solution. Based on skewness statues, the typical ANSYS mesh quality shows (0.5 to 0.8) as a satisfactory result, and the researcher achieves (0.79) mesh quality.

Step 4**:** define the applied loads

Before or after finite element meshing, the applied loads can be specified directly on the solid model. All elements with structural degrees of freedom and mass are subject to inertial loads (gravity, spinning, etc.). There are two sorts of load-applying methods: Direct loads, which are applied directly to the elements but may be imposed at nodes, and nodal loads, which can be applied at nodes but are not directly related with the elements. The D and F commands are used to input nodal loads, which are linked to the degrees of freedom at the node. An element may employ either the nodal or element loading forms, with the element loading format having priority. Element loads are the third kind of load. KEYOPTs (key options) are used to modify the behavior, formulation, and output of various beam and shell components. The most significant input element is the KEYOPT, which should be carefully chosen. The KEYOPTs may govern stress states, different elements have different options for how they can be made, how they can be printed, how they can be output, how they can be loaded, and how they can be heated, depending on what kind of element they are. The detailed explanation of each element type includes a broad definition of each KEYOPT. Because KEYOPTs may be combined, there is a lot of flexibility in fine-tuning the element type to meet a specific case. Figure 3.11 shows how this method is used on a slab plane.

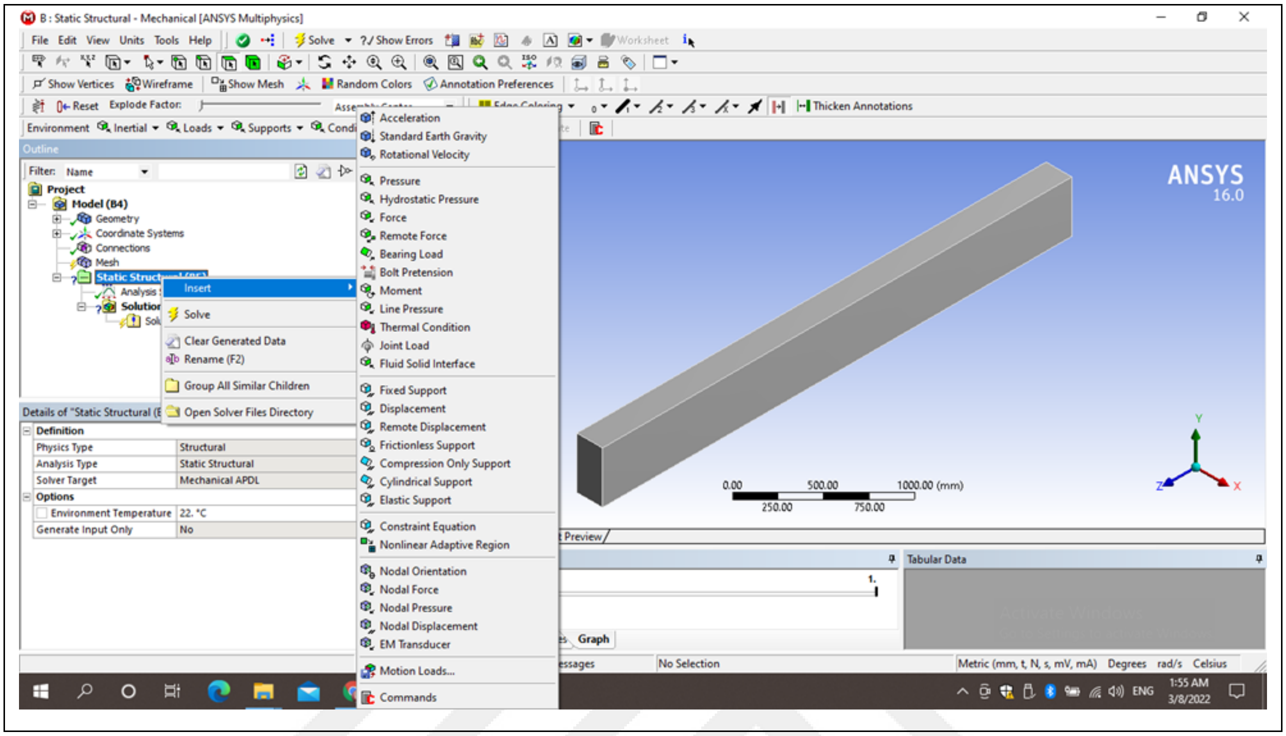

Figure 3. 11: Applied Load on Slab Elements

3.9 SOLVING PROCESS

When the solution calculations are applied, the solid model loads are immediately transferred to the finite element model. As demonstrated in Figure 3.12, the SOLVE command entails (Main Menu> Solution> Solve> Current LS).

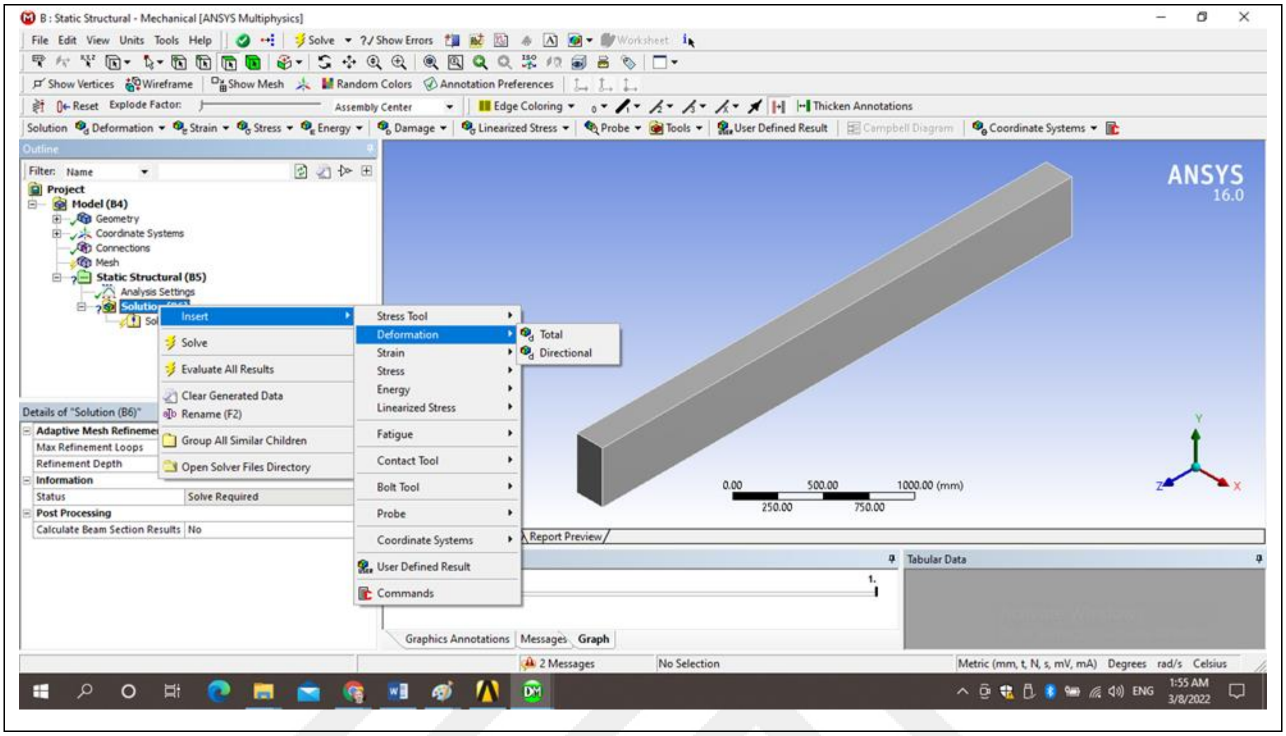

Figure 3. 12: ANSYS SOLVE Command

The model creation, which includes meshing, is finished after preprocessing. The solution phase is presented by ANSYS. During the solution process, ANSYS allows you to pick specific choices. Analysis Options or Solution Controls are used to specify them. Users can use APDL commands to map stresses from an ANSYS APDL model to the receiving model and examine the mapped stress values. It can solve by constraining all degrees of freedom in the receiving model, removing any extraneous loads, and constraining all degrees of freedom in the receiving model. The mapped stress values should be accessible to list and display as results over the model if the material characteristics are linear.

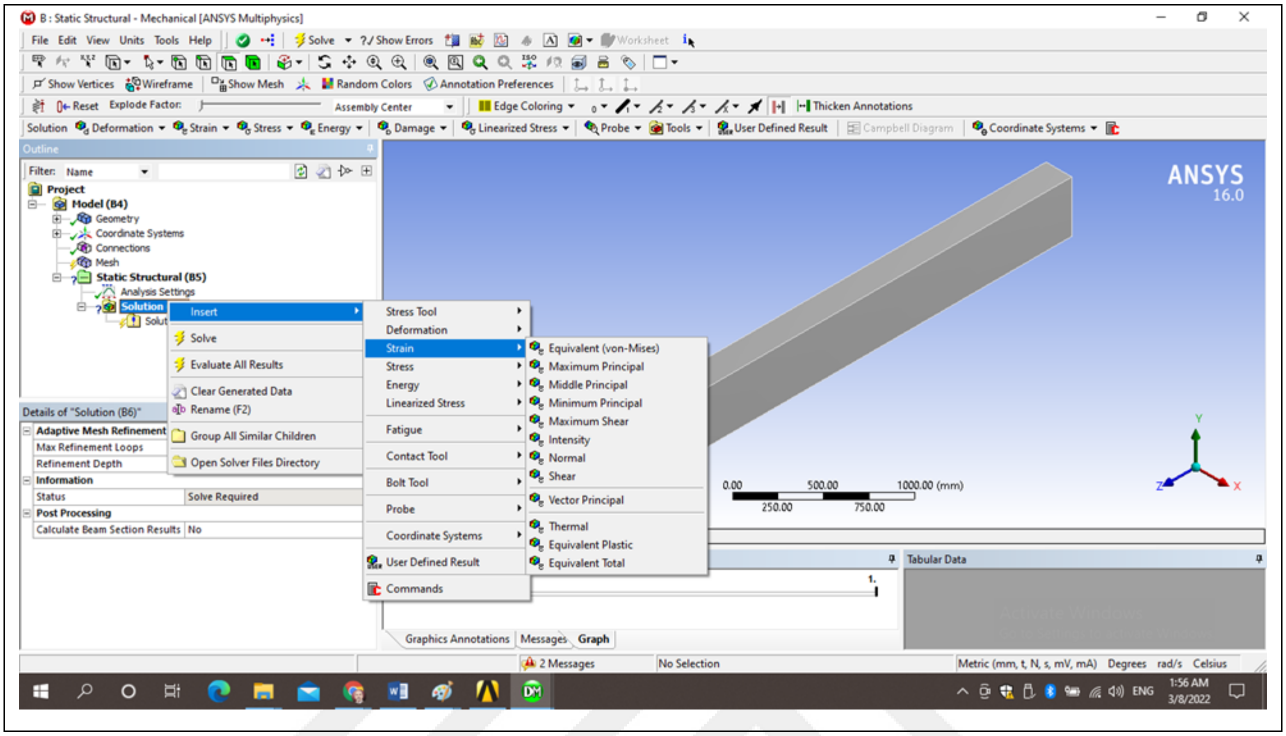

Figure 3. 13: Stress Command in ANSYS SOLVER

4. RESULTS AND DISCUSSION

In this chapter, numerical evaluations were performed on three distinct types of beams selected from the available experimental research. This chapter also describes how to develop a numerical 3-D model and input material data to simulate the nonlinear behavior of beams subjected to an elastic foundation, as well as how to compare the behavior of polypropylene fiber reinforced beams.

4.1 THE CASE STUDIES

The experiments were conducted based on two groups conditions, the first of which was traditional reinforced concrete and the second of which was polypropylene fiber reinforced, as shown in table 4.1 and Figures 4.1 to 4.3. The experiments were conducted based on two groups conditions, the first of which was traditional reinforced concrete and the second of which was polypropylene fiber reinforced. The first group had 12 mm of reinforcement, whereas the second had the same beam form but with polypropylene fiber reinforcement.

Table 4. 1: The dimensions of the used samples

Beam Type	Width	Height	Length
1	500	600	6500
2	200	400	3000

The experimental program can be described as follows: the main parameters are the volume fraction of polypropylene fiber reinforcement, for that, the researcher tested the concrete based on two conditions, the first condition is the traditional concrete and the second test is the polypropylene fiber reinforcement concrete.

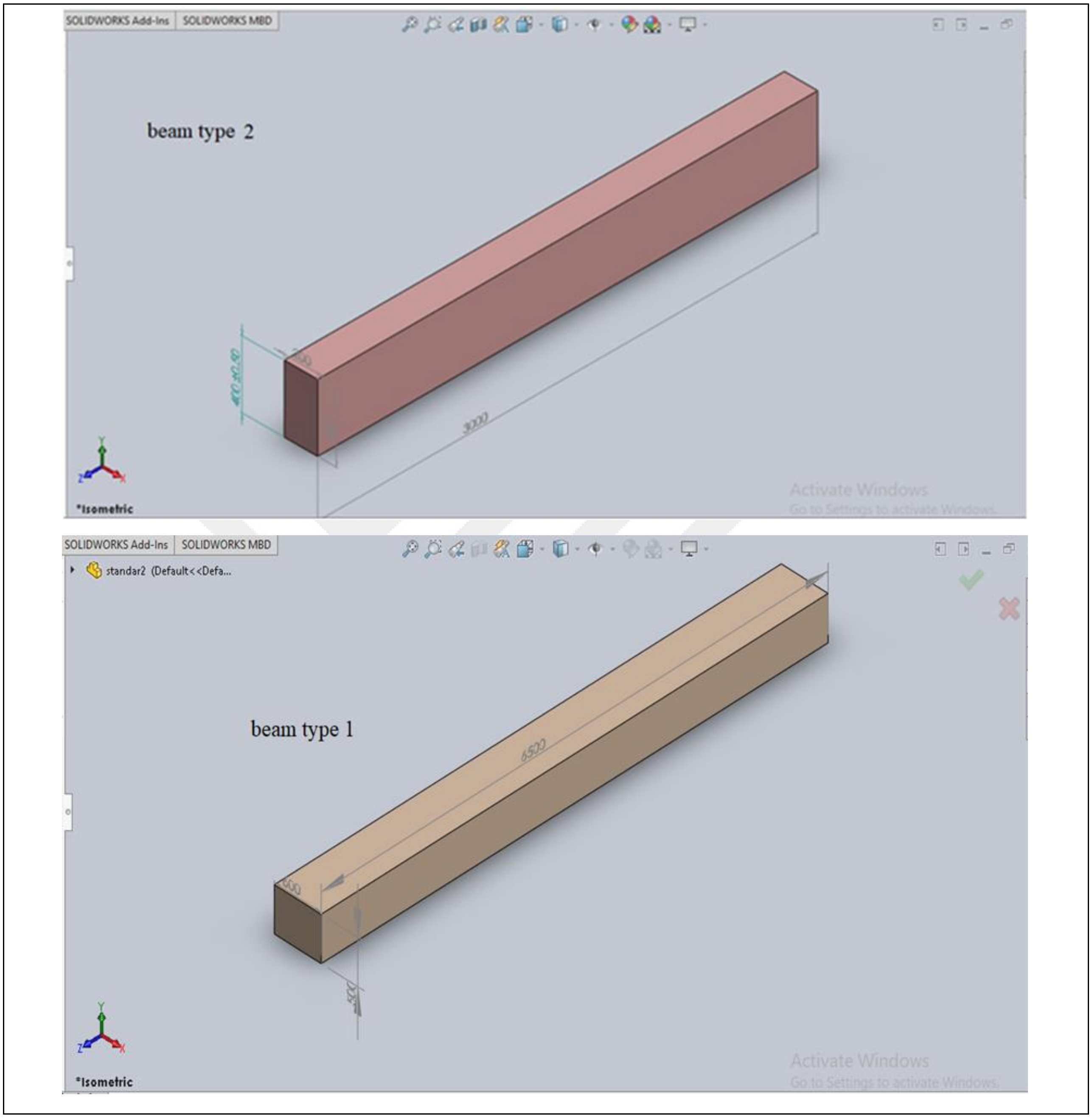

Figure 4. 1: Beam Type (1) and Beam Type (2)

The laboratory test results will be applied and subjected to ANSYS simulation software to find out the differences. Total of twenty-four simulation test are suggested for investigation as in Table 4.1.

Table 4. 2: Total of Twenty-Four Simulation Test are Suggested for Investigation

Test code	concrete conditions	Type of beam	Elastic Foundation conditions (KN/mm3)	Load (KN)
Z 1-1	Traditional concrete	Type 1	K=100	30, 70,120
Z 1-2	Traditional concrete	Type 2	K=150000	30, 70,120
Z 2-1	concrete with polypropylene	Type 1	K=100 to 400000	30, 70,120
Z 2-2	concrete with polypropylene	Type 2	K=100 to 400000	30, 70,120

The results of the two types of concrete spacemen's can be shown in Figure 4.2 in sequent for all tested specimens. Also, compressive strength results of each type are presented in Table 4.2

Figure 4. 2: The Results of the Two Types of Concrete Spacemen's

Table 4. 3: Properties for Reinforced and Concrete Compressive Stress

The yield stress of flexural reinforced (MPa)	480
The yield stress of shear reinforced (MPa)	421
The 28 days compressive stress of concrete f'_c (MPa)	32.520
The 28 days compressive stress of concrete with polypropylene fiber reinforced (Vf:0.75) f'_c (MPa)	40.453

4.2 VERIFICATION AND VALIDATION

The study's validation and verification are presented in this part. Based on the test circumstances of a prior study, the concrete beam is modelled. The experimental data gained is used to validate the models in this work, as well as to select an acceptable model with a right model configuration and a suitable mesh technique that can be constructed and employed on the boundary condition of interest. The findings of all of this research show how to develop a correct model and also how to explain concrete behavior based on the chosen model.

4.2.1 Model Validation

The validation approach utilized by comparing the findings based on particular chosen model is used to guarantee that the structural simulation model is developed in the proper circumstances and will be solved in a good representation of reality.

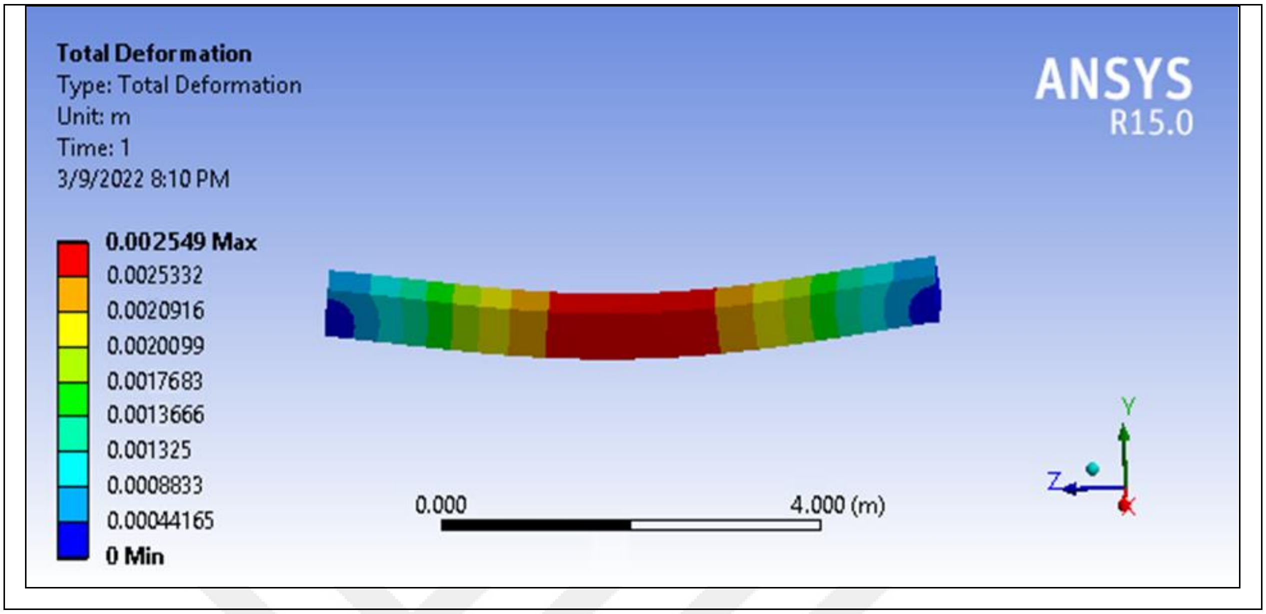

Figure 4. 3: Static Structure Result

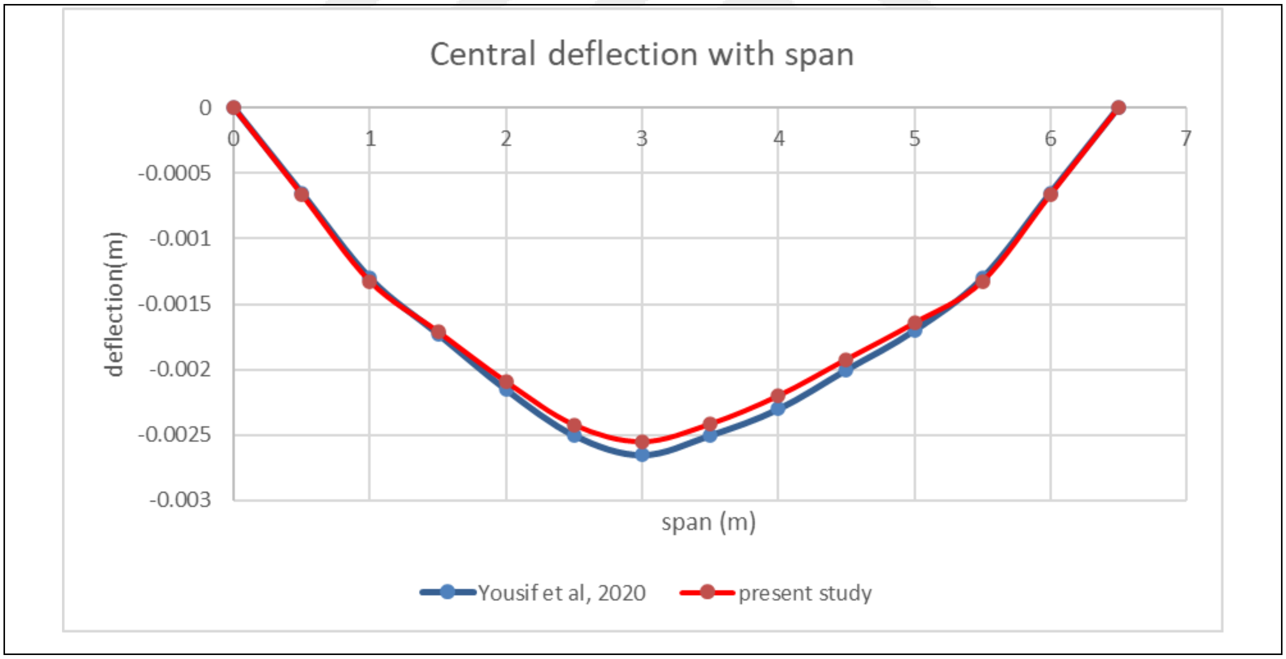

Figure 4. 4: Plot the test results for both of Yousif et al, 2020 with the present results

The results of the FE analysis are generally consistent with the expected behavior, namely that the deflection of a beam resting on an elastic foundation is a function of the subgrade modulus of the soil, and that the relationship between deflection and subgrade modulus of the soil is clear (see Figures). In addition, when the applied load (load – step) increases, the deflection increases. In any case, the FE method can accurately forecast the structural behavior of beams sitting on elastic foundations, making it useful in professional engineering work. The proposed model may be used to beams on elastic foundations with any form of common boundary and contact unilateral circumstances or loading combinations. It is also possible to evaluate the impact of the environment on the settling of the beams.

Table 4. 4: comparative results between the present study and previous study

span (m)	Yousif et al, 2020	present study	error %
0	0	0	
0.5	-0.00065	-0.0006625	1.92%
1	-0.0013	-0.001325	1.92%
1.5	-0.001725	-0.00170805	0.98%
2	-0.00215	-0.0020911	2.74%
2.5	-0.0025	-0.00242005	3.20%
3	-0.00265	-0.002549	3.81%
3.5	-0.0025	-0.002414	3.44%
4	-0.0023	-0.002199	4.39%
4.5	-0.002	-0.001921	3.95%
5	-0.0017	-0.001643	3.35%
5.5	-0.0013	-0.001325	1.92%
6	-0.00065	-0.0006625	1.92%
6.5	0	0	

4.3 SIMULATE LONG SPAN BEAM

The initial step of 3D modelling involves creating volume by dimensions for concrete body. Due to symmetry in both members' geometries, steel supports and reinforcements, a half of them will be modeled, which will be used for the FE analysis. This requires applying additional boundary constrains, perpendicular to the axis of symmetry.

4.3.1 Comparison between Load Deflection for Long Span Beam when k=50000

This section shows the typical load versus deflection characteristics of a concrete beam. The model deflections vertical displacements are measured in the Y-direction, at the center of the bottom face of the FE model, displaying Uy. The applied load is represented by the vertical axis in kN, while the deflection is represented by the horizontal axis in mm. The load vs. displacement curve is used to compare solid and hollow beam findings with experimental laboratory results.

Figures 5. 4 to 5. 9 show the difference between a typical concrete beam and a polypropylene-reinforced concrete beam in 3D FE Model analysis, and all load-deflection curves for the tested beam exhibit identical behavior. In comparison with the experimental values, all the FE numerical models approximately display large deflection at the ultimate stage.

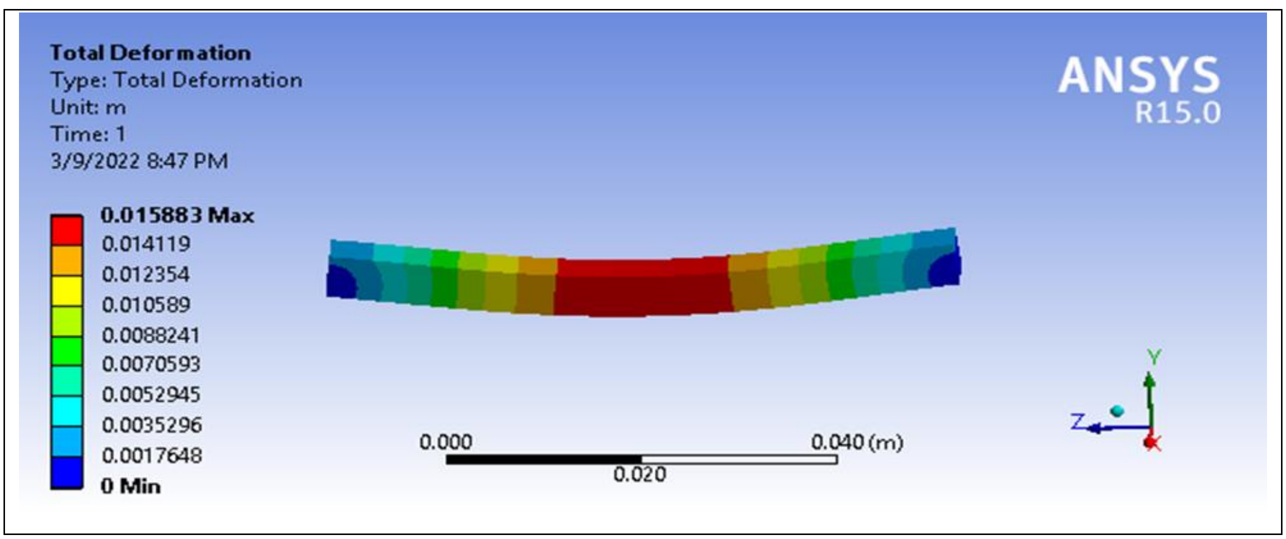

Figure 4. 5: results of total deformation of concrete for long span beam when k=50000

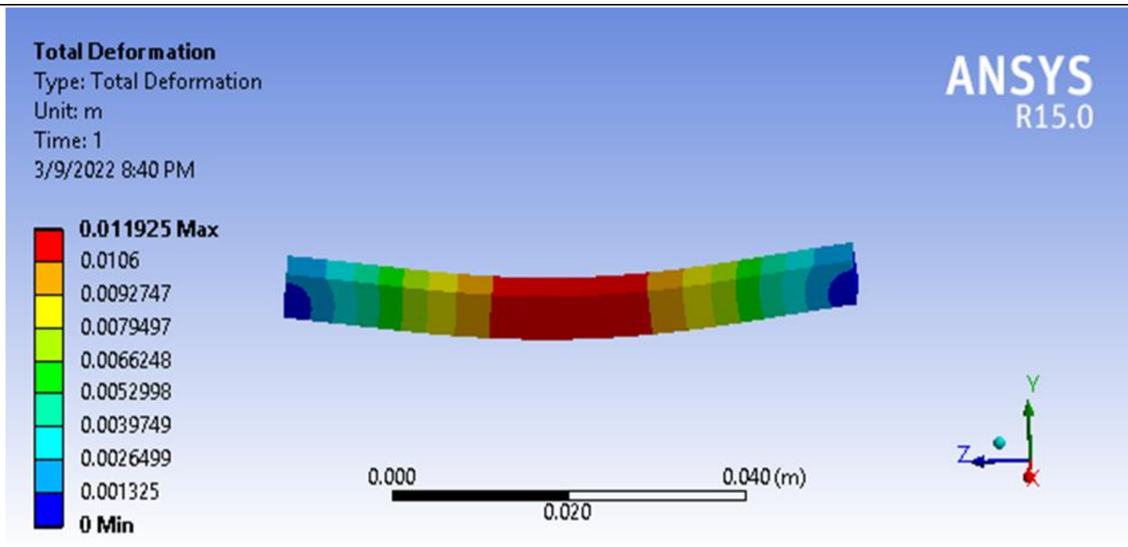

Figure 4. 6: results of total deformation of PFRC for long span beam when k=50000

The load – deflection curves from the FE research 3D FE model accord well with lab test data from the experimental for the RC solid beam SB 100. The load – deflection curves match well for both experimental and FE analysis 3D FE Model, after which the FE analysis 3D FE Model deflections curves are bigger than the experimental deflections curves. The end load of the FE analysis 3D FE Model is 64400 N, which is higher than the experimental final load of 60000 N. The load – deflection curves from FE analysis 3D FE Model correspond well with the data recording from literature for the RC solid beam SB 50. The relationship of load – deflection are similar for both experimental, after which the deflections curves from FE analysis 3D FE Model become less than the deflections curves from experimental

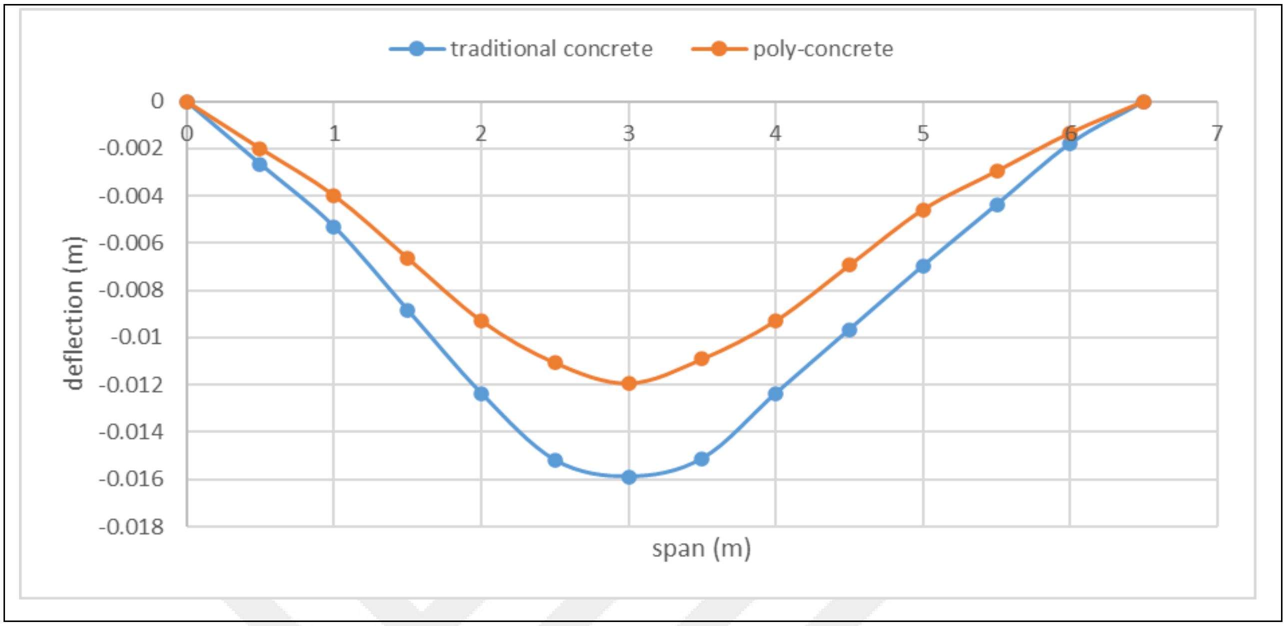

Figure 4. 7: comparison of total deformation of concrete based on different concrete for long span beam when k=50000

4.3.2 Comparison between Load Deflection for Long Span Beam when k=150000

The evenly distributed applied load (120 kN/m) represents a load applied to the beam from the wall (represent foundation). To get and receive data for deflection variation with step applied load, the load is applied in steps (i.e. ratio from 120 kN/m). The foundation is modeled as Winkler with varying subgrade modulus to observe how beam deflection changes with subgrade modulus (ratio of soil bearing capacity to settlement) equal to 150000 kN/m3. 15 a different thorough comparison between maximum deflections in two situations is provided in Figure 5. The maximum deflection was observed at mid-span of beam at the center of the bottom face, which is on the lower side from the beam members. The centerline deflection from numerical model were compared with the experimental data, are shown in Figure 5. 15 a separate detailed comparison between maximum deflections in two cases. Additional results generated by the FE are presented, and also observed that the difference between the maximum deflection results of lab test and FE numerical models ranging from about 15 mm and it is a good to a great extent.

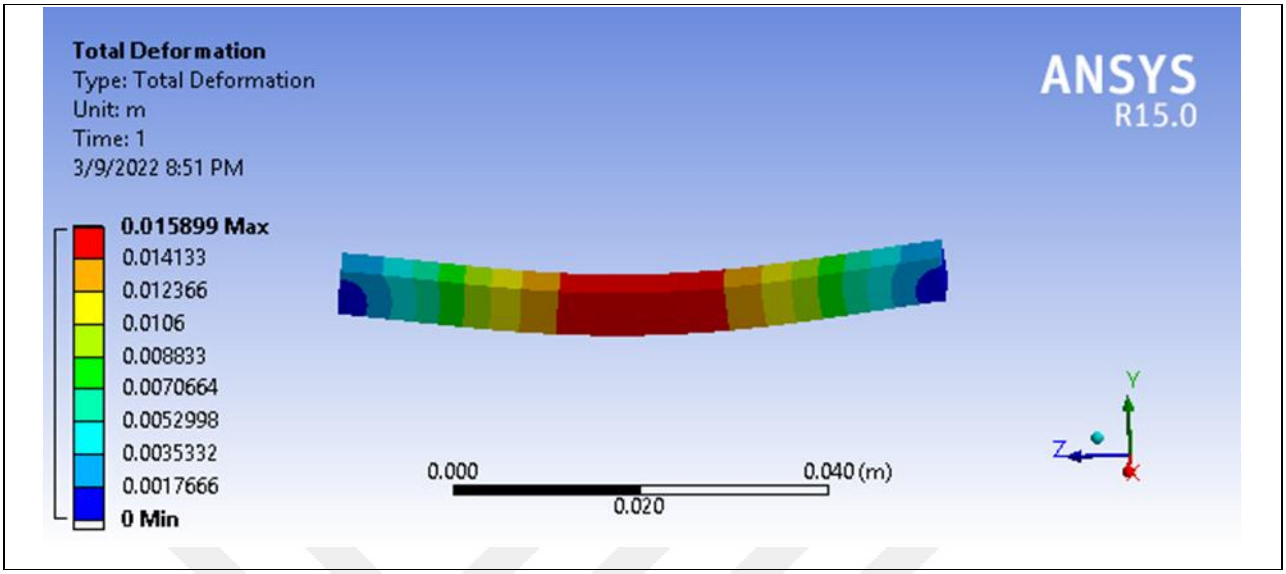

Figure 4. 8: results of total deformation of concrete for long span beam when k=150000

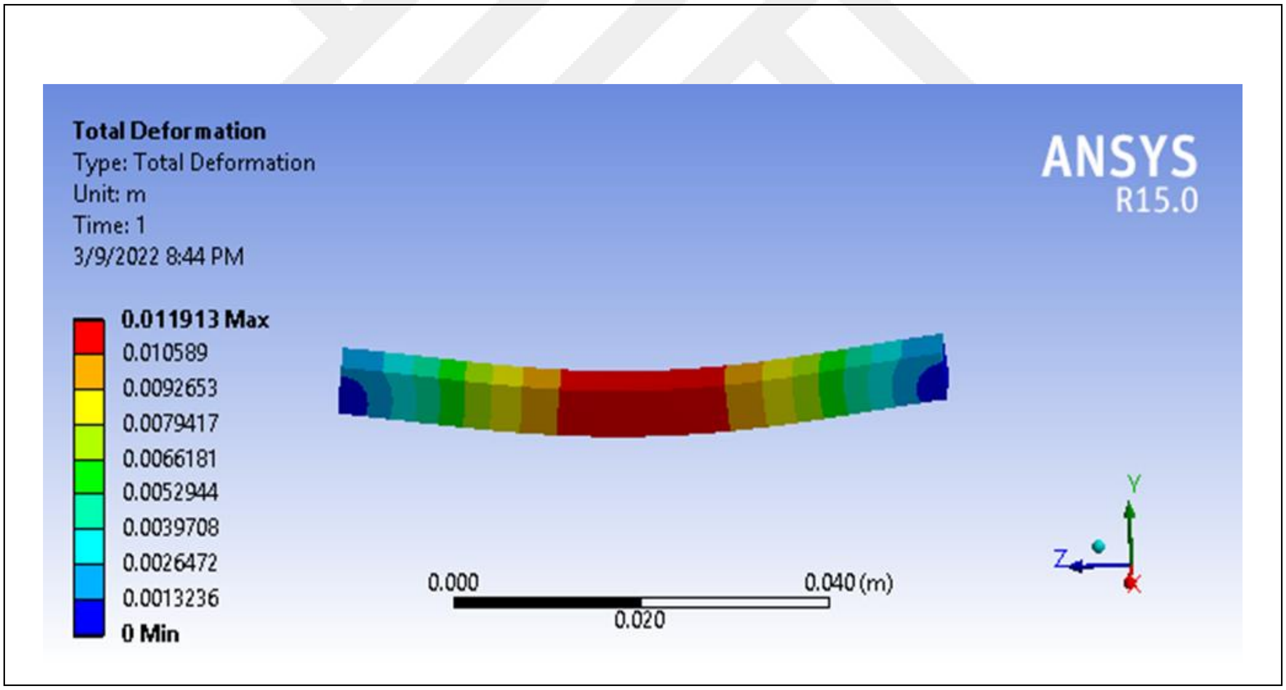

Figure 4. 9: results of total deformation of PFRC concrete for long span beam when k=150000

The largest deflection was recorded in the center of the bottom face, which is on the lower side from the beam members, in the mid-span of a concrete beam. The numerical model's centerline deflections were compared between traditional concrete and concrete with polypropylene fibre reinforced beams, as shown in Figure 5. 15 a separate comprehensive comparison between maximum deflections in two scenarios. Additional FE findings are shown, and it is also noted that the difference between maximum deflection values ranges from around 5 mm and is good to a large extent.

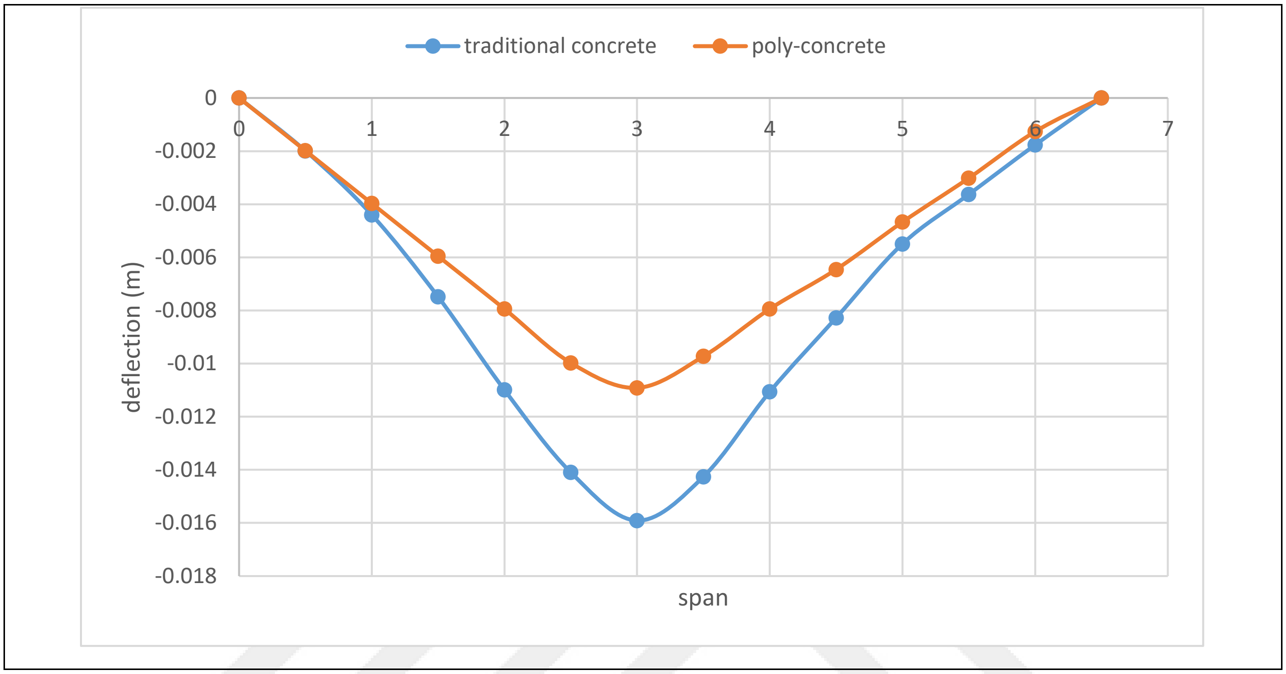

Figure 4. 10: comparison of total deformation of concrete based on different concrete for long span beam when k=150000

The load – deflection curves for varying Subgrade modulus (k) from FE 3D are shown in Figures 5. 6 and 5. 9. The results obtained from the lab test for the concrete beam matches extremely well with FE Models, and the behavior of the numerical models in load – deflection curves was also observed. This is due to several elements at the forefront of precision at the simulation work and a suitable decision for the right density of meshing distribution. It is similar to the disposition of classic concrete reinforced beam and polypropylene fibre reinforced beam beams. For both examples, the load – deflection curves are comparable, however the deflections curves from the FE model are bigger than the deflections curves from the experimental.

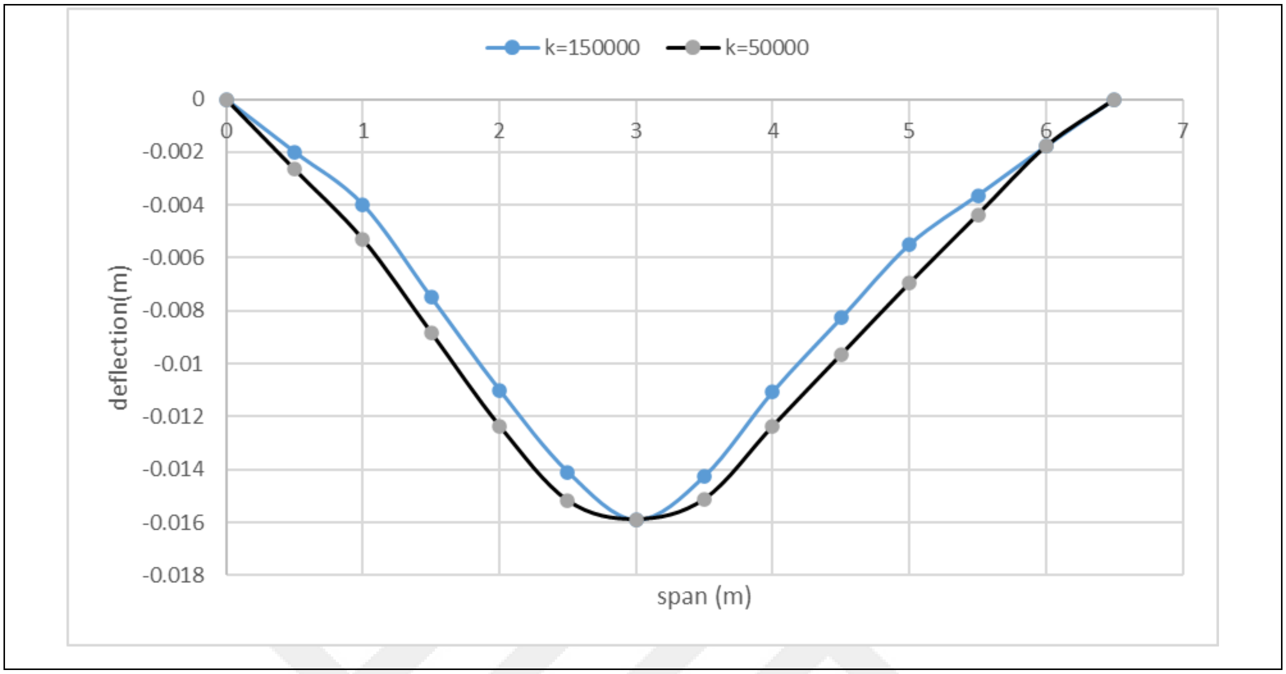

Figure 4. 11: comparison of total deformation of concrete based on different Ks for long span beam

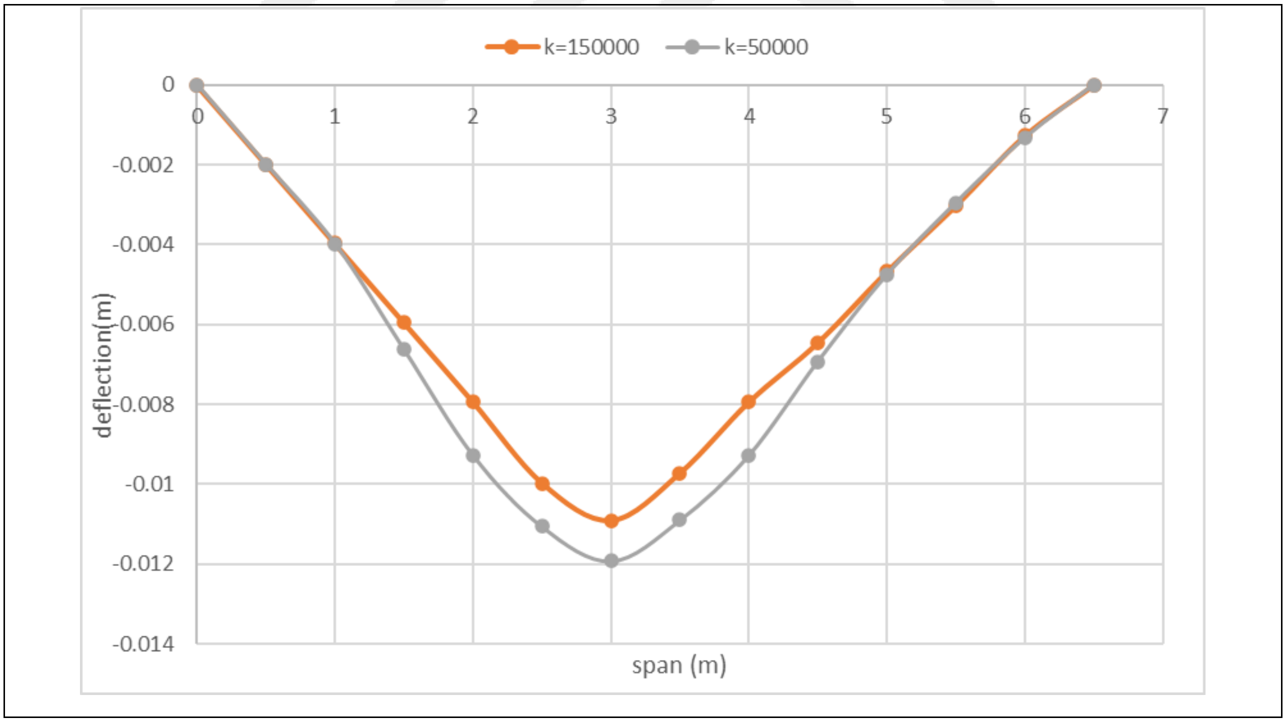

Figure 4. 12: comparison of total deformation of PFRC concrete based on different Ks for long span beam

4.4 SIMULATE SHORT SPAN BEAM

The next step of 3D modelling involves creating volume by dimensions for short span concrete body. Due to symmetry in both members' geometries, steel supports and reinforcements, a half of them will be modeled, which will be used for the FE analysis. This requires applying additional boundary constrains, perpendicular to the axis of symmetry.

4.4.1 Comparison between Load Deflection for Short Span Beam when k=50000

The difference between traditional concrete beam and beam reinforced with polypropylene in 3D FE Model for short span analysis is illustrated in Figure 5. 4 to Figure 5. 9, and all load-deflection curves for the tested beam have similar behavior. In comparison with the experimental values, all the FE numerical models approximately display large deflection at the ultimate stage.

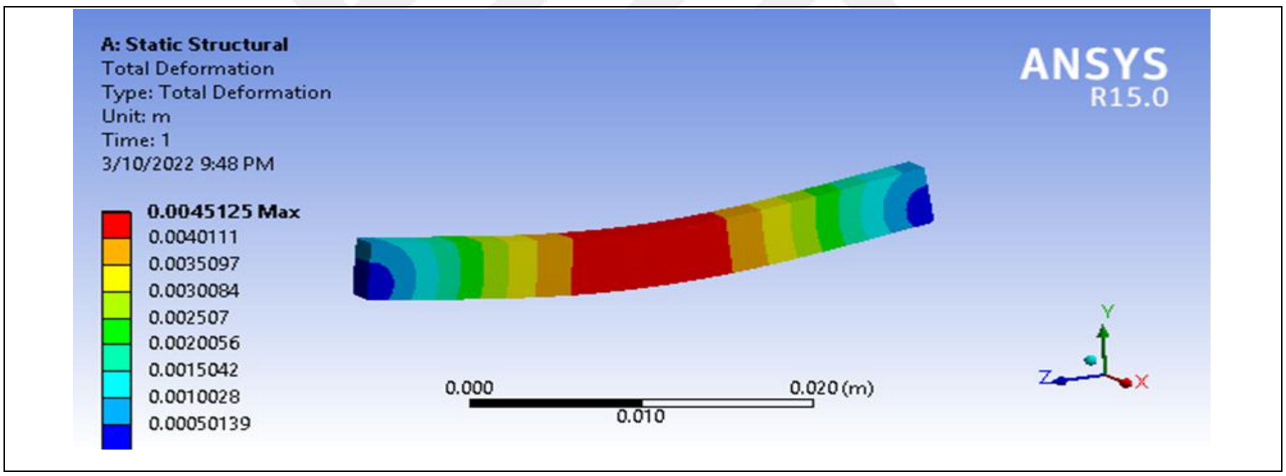

Figure 4. 13: results of total deformation of concrete for short span beam when k=50000

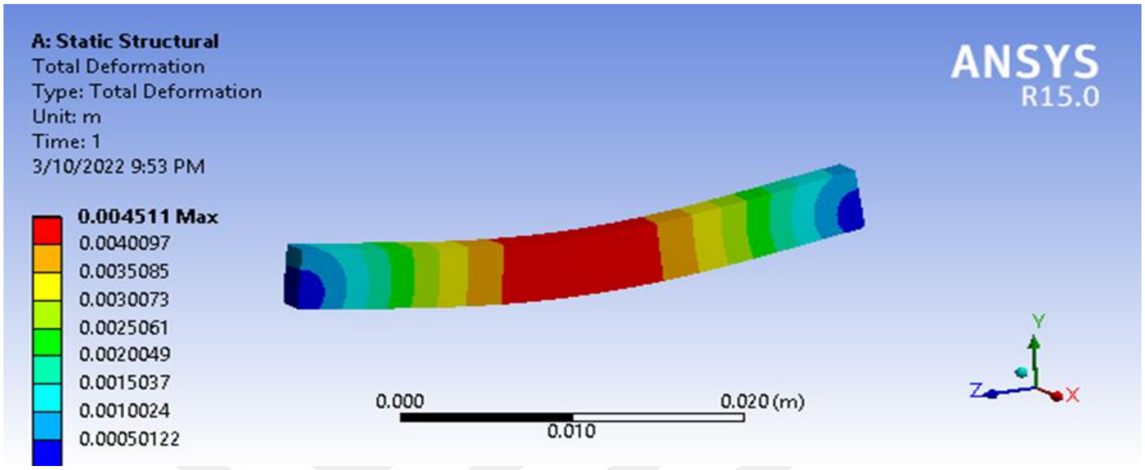

Figure 4. 14: results of total deformation of concrete for short span beam when k=50000

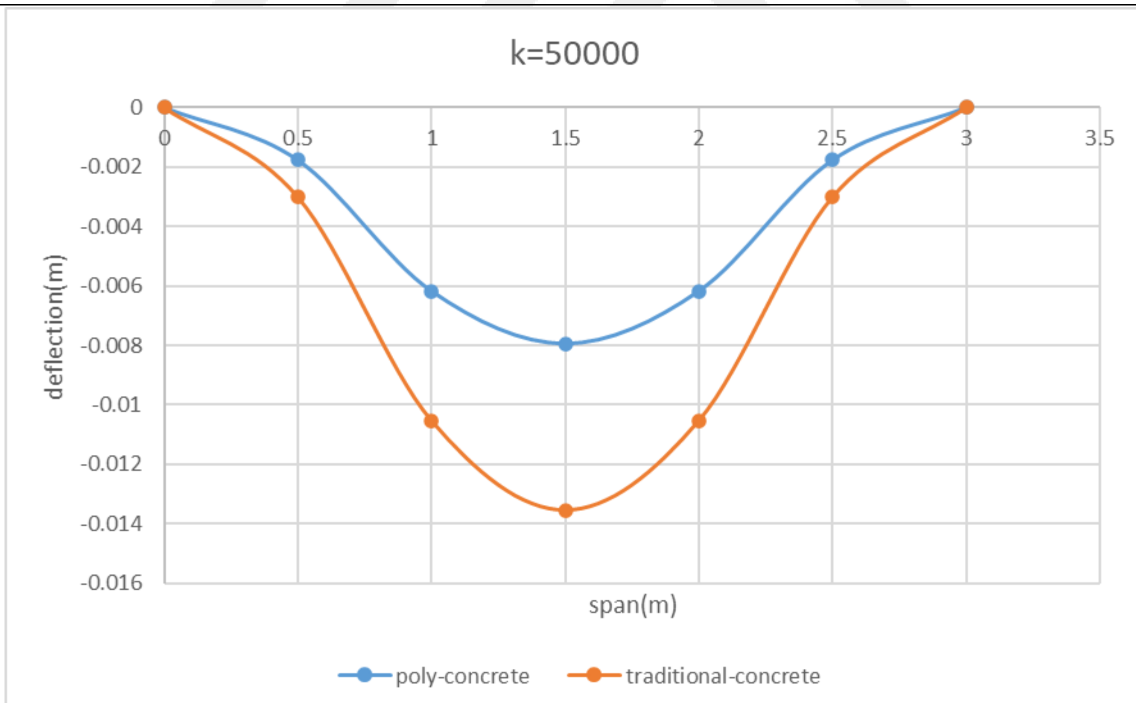

Figure 4. 15: comparison of total deformation of concrete based on different Ks for short span beam when k=50000

4.4.2 Comparison between Load Deflection for Short Span Beam when k=150000

The uniformly distributed applied load is (120 kN/m) represent a load come from wall and applied to the beam (represent foundation). The load is applied as step (i.e. ratio from120 kN/m) to obtain and get results for deflection variation with step applied load. The foundation is modeled as Winkler with varying subgrade modulus to observe how beam deflection changes with subgrade modulus (ratio of soil bearing capacity to settlement) equal to 150000 kN/m3. The largest deflection was recorded in the center of the bottom face, which is on the lower side of the beam, in the mid-span of the beam. The numerical model's centerline deflection was compared to experimental data, with a separate comprehensive evaluation of maximum deflections in two examples. Additional FE data are shown, and it is also noted that the discrepancy between the maximum deflection results of lab tests and FE numerical models is around 15 mm, and it is good to a large extent.

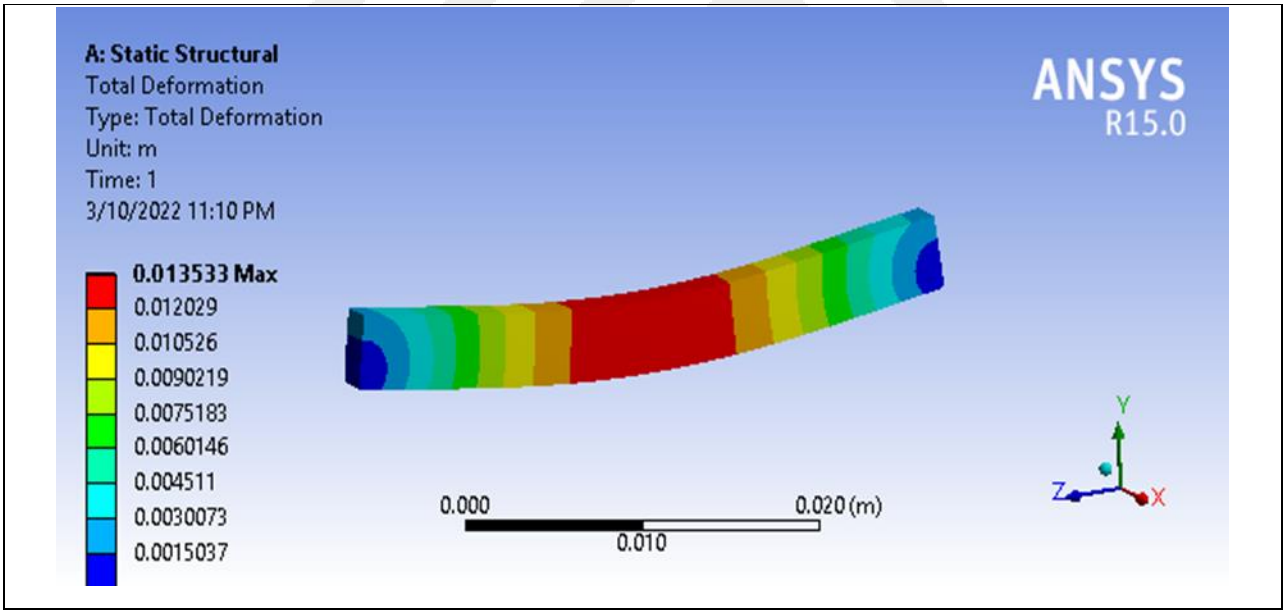

Figure 4. 16: results of total deformation of concrete for short span beam when k=150000

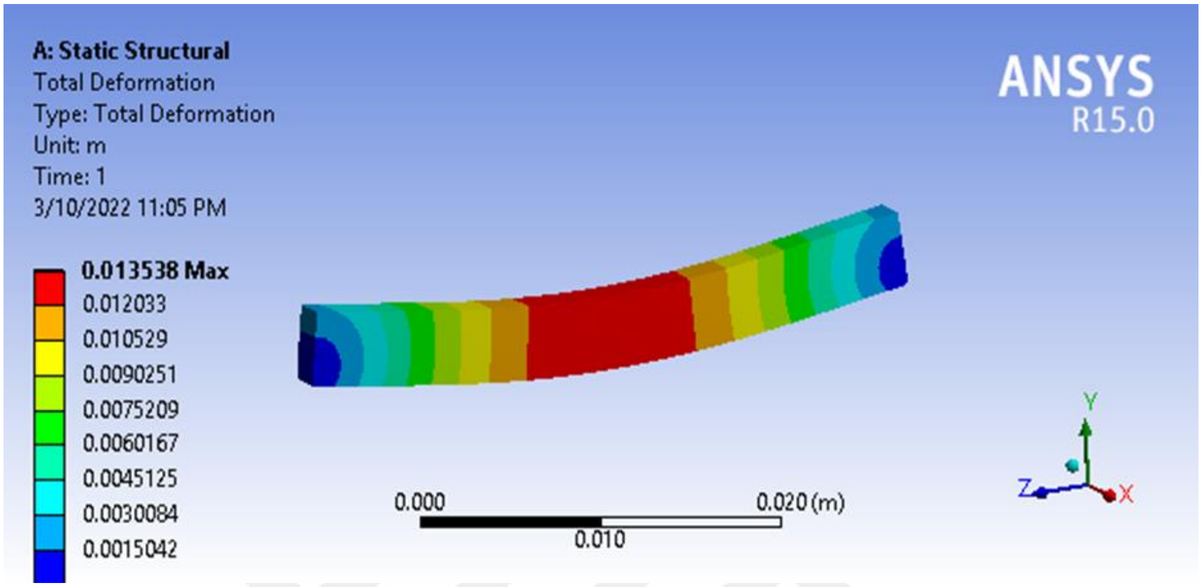

Figure 4. 17: results of total deformation of concrete for short span beam when k=150000

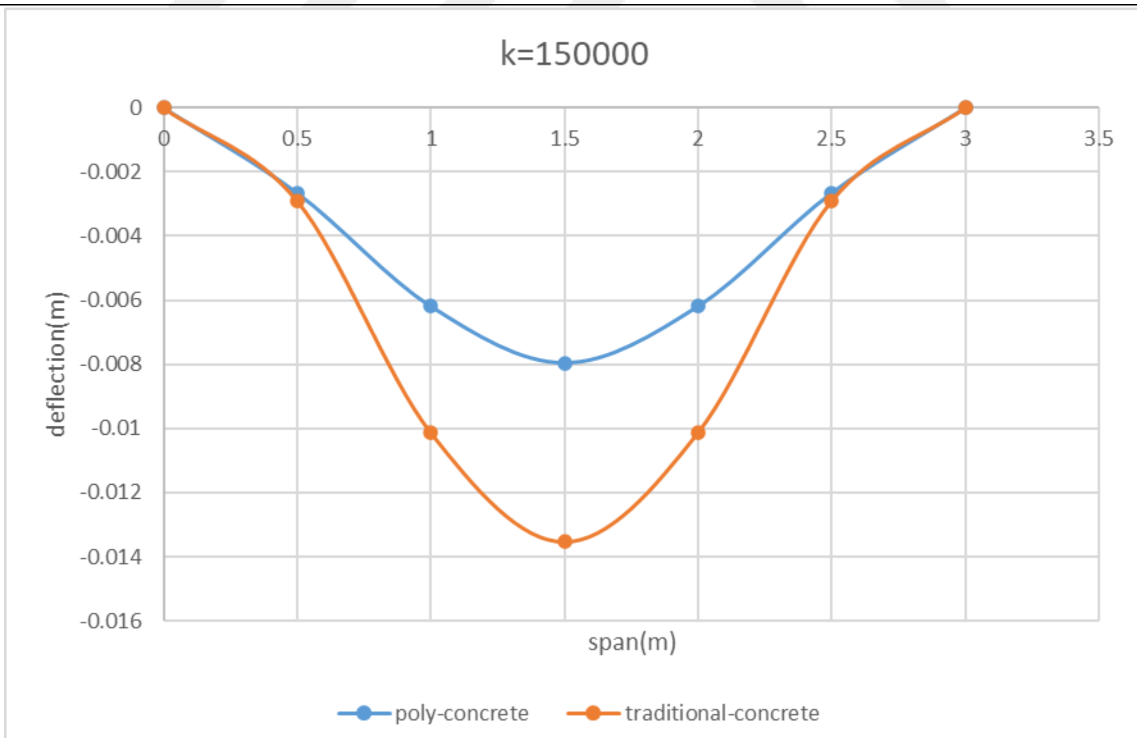

Figure 4. 18: comparison of total deformation of concrete based on different Ks for short span beam when k=150000

The largest deflection was recorded in the center of the bottom face, which is on the lower side from the beam members, in the mid-span of a concrete beam. The numerical model's centerline deflections were compared between traditional concrete and concrete with polypropylene fibre reinforced beams, as shown in Figure 5. 15 a separate comprehensive comparison between maximum deflections in two scenarios. Additional FE findings are shown, and it is also noted that the difference between maximum deflection values ranges from around 5 mm and is good to a large extent.

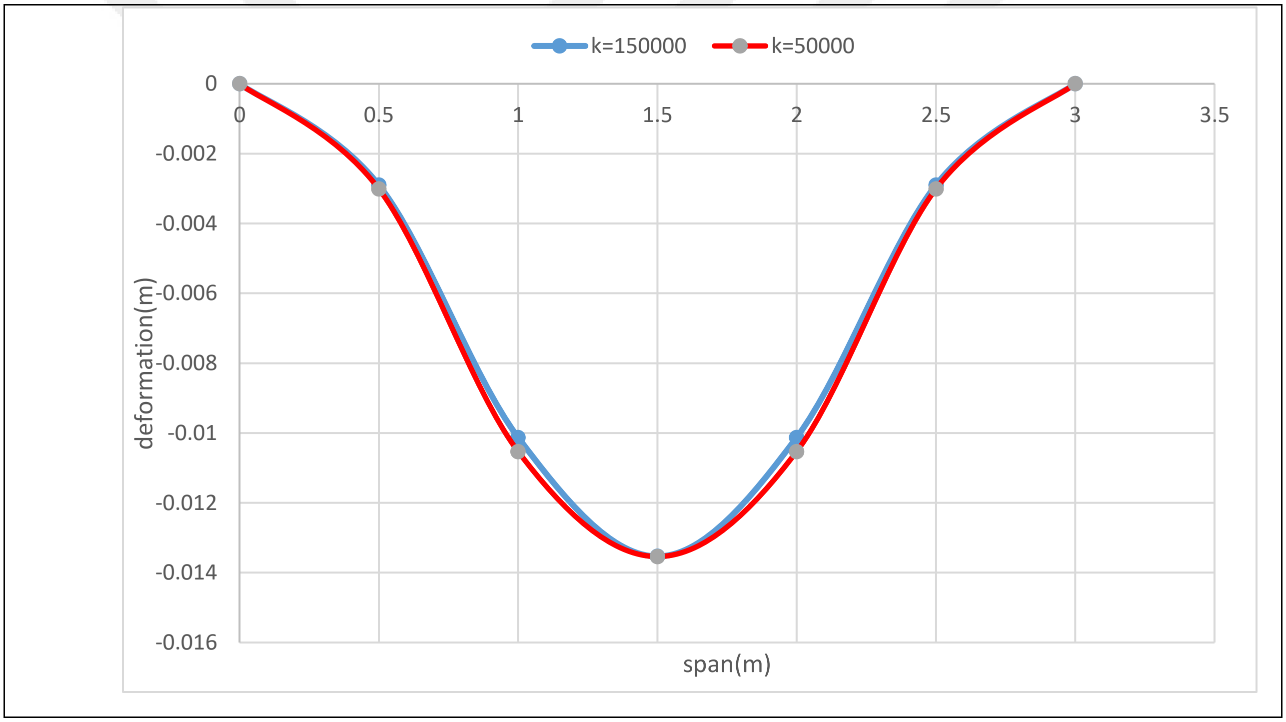

Figure 4. 19: comparison of total deformation of concrete based on different Ks for short span beam

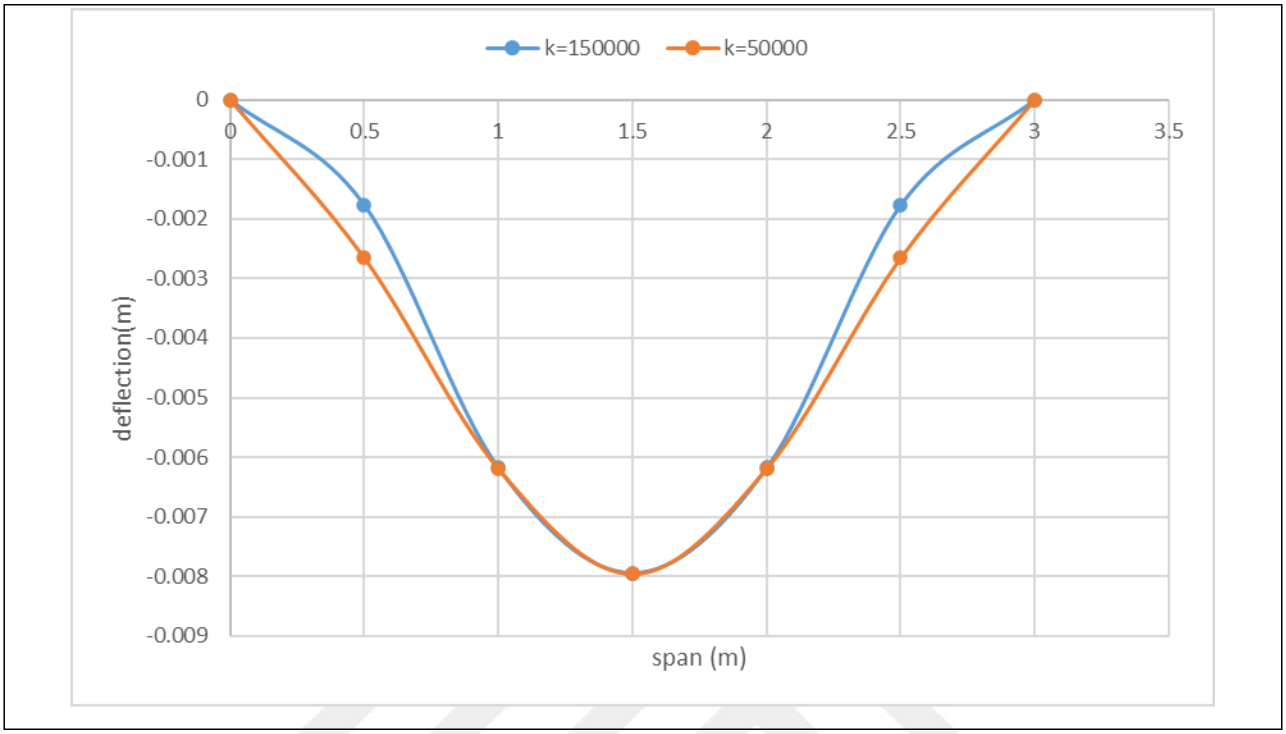

Figure 4. 20: comparison of total deformation of PFRC concrete based on different Ks for short span beam when k=50000

The load – deflection curves for varying Subgrade modulus (k) from FE 3D are shown in Figures 5. 6 and 5. 9. The results obtained from the lab test for the concrete beam matches extremely well with FE Models, and the behavior of the numerical models in load – deflection curves was also observed. This is due to several elements at the forefront of precision at the simulation work and a suitable decision for the right density of meshing distribution. It is similar to the disposition of classic concrete reinforced beam and polypropylene fibre reinforced beam beams. For both examples, the load – deflection curves are comparable, however the deflections curves from the FE model are bigger than the deflections curves from the experimental.

5. CONCLUSION AND RECOMMENDATION

This chapter summarizes the research methodology's accomplishments as well as efforts to fill research gaps. Using ANSYS software, this work presents a sequence of operations and conditions for processing a reinforced concrete beam case study. The evaluation of the differences between a concrete beam and a polypropylene-reinforced beam is the study's key contribution. The purpose of this thesis is to determine the deflection behavior of a beam when different loads are applied to it and it is exposed to varied subgrade modulus effects. The subgrade modulus ranged from (50000 to 150000) kN/m3 and the selected load was 120 KN. The following concerns may be deduced from the current work:

a) The FE analytical tests carried out for the two cases studied indicate that response to the load and deflection and the ultimate loads behavior in concrete beams are in very well agreement.
b) The optimum enchainment obtained when the polypropylene fiber added to the beam concrete with high load effect
c) The optimum enchainment obtained in booth short length and long beam length with the same enhancement behavior of adding the polypropylene fiber.

5.1 FUTURE WORKS

In the ongoing research, a new investigation for concrete material needs for exposing the booth types on high temperature based on different beam design conditions.

REFERENCES

[1] Z. Y. Ai, Z. X. Li, and Y. C. Cheng, “BEM analysis of elastic foundation beams on multilayered isotropic soils,” *Soils Found.*, vol. 54, no. 4, pp. 667–674, 2014, doi: 10.1016/j.sandf.2014.06.008.

[2] M. I. Nadagouda and G. Ravi, “Analytical study on Flexural behaviour of RCC slabs with concealed beams using ANSYS,” *Int. Res. J. Eng. Technol.*, vol. 4, no. 7, pp. 3094–3101, 2017, [Online]. Available: https://irjet.net/archives/V4/i7/IRJET-V4I7622.pdf.

[3] Z. Y. Ai, Z. X. Li, and Y. C. Cheng, “BEM analysis of elastic foundation beams on multilayered isotropic soils,” *Soils Found.*, vol. 54, no. 4, pp. 667–674, 2014, doi: 10.1016/j.sandf.2014.06.008.

[4] J. Mackerle, “Finite element vibration analysis of beams, plates and shells,” *Shock Vib.*, vol. 6, no. 2, pp. 97–109, 1999, doi: 10.1155/1999/692380.

[5] E. Rahman, “STUDY OF THE EFFECT OF ELASTIC FOUNDATION ON THE ACCELERATED DURABILITY TESTING OF Master of Science,” 2016.

[6] K. Frydrýšek, R. Jančo, and H. Gondek, “Solutions of beams, frames and 3D structures on elastic foundation using FEM,” *Int. J. Mech.*, vol. 7, no. 4, pp. 362–369, 2013.

[7] S. Brischetto, “Three-dimensional exact free vibration analysis of spherical, cylindrical, and flat one-layered panels,” *Shock Vib.*, vol. 2014, 2014, doi: 10.1155/2014/479738.

[8] T. Karamanski and K. Kazakov, “Modified model of a plate based on the Winkler foundation,” *Comput. Methods Exp. Meas. XII*, vol. 41, pp. 417–423, 2005.

[9] T. M. Al-hussaini, “SOIL-FOUNDATION-STRUCTURE INTERACTION ANALYSIS.”

[10] S. N. Akour, “Dynamics of nonlinear beam on elastic foundation,” *WCE 2010 - World Congr. Eng. 2010*, vol. 2, no. June 2010, pp. 1427–1433, 2010.

[11] X. Wang, W. Li, J. Yao, Z. Wan, Y. Fu, and T. Sheng, “Free vibration of functionally graded sandwich shallow shells on winkler and pasternak foundations with general boundary restraints,” *Math. Probl. Eng.*, vol. 2019, 2019, doi: 10.1155/2019/7527148.

[12] M. Khalifa, “Effects of non-uniform Winkler foundation and non-homogeneity on the free vibration of an orthotropic elliptical cylindrical shell,” *Eur. J. Mech. A/Solids*, vol. 49, no. February 2015, pp. 570–581, 2015, doi: 10.1016/j.euromechsol.2014.09.009.

[13] L. Xu *et al.*, “Experimental Investigation on Damage Behavior of Polypropylene Fiber Reinforced Concrete under Compression,” *Int. J. Concr. Struct. Mater.*, vol. 12, no. 1, 2018, doi: 10.1186/s40069-018-0302-3.

[14] R. Y. Kumar, K. Vinobalaji, and M. N. Prasad, “Experimental investigation of hollow core slab using different fibre,” *Int. J. Civ. Eng. Technol.*, vol. 9, no. 11, pp. 1199–1206, 2018.

[15] Q. Liu and J. Ma, “Analytical Model for Beams on Elastic Foundations Considering the Coupling of Horizontal and Vertical Displacements,” *J. Eng. Mech.*, vol. 139, no. 12, pp. 1757–1768, 2013, doi: 10.1061/(asce)em.1943-7889.0000635.

[16] A. T. Daloglu and C. V. G. Vallabhan, “ Values of k for Slab on Winkler Foundation ,” *J. Geotech. Geoenvironmental Eng.*, vol. 126, no. 5, pp. 463–471, 2000, doi: 10.1061/(asce)1090-0241(2000)126:5(463).

[17] Z. P. Mourelatos and M. G. Parsons, “A finite element analysis of beams on elastic foundation including shear and axial effects,” *Comput. Struct.*, vol. 27, no. 3, pp. 323–331, 1987, doi: 10.1016/0045-7949(87)90055-1.

[18] D. Dinev, “Analytical Solution of Beam on Elastic,” *Eng. Mech.*, vol. 19, no. 6, pp. 381–392, 2012.

[19] S. M. Binesh, “Analysis of beam on elastic foundation using the radial point interpolation method,” *Sci. Iran.*, vol. 19, no. 3, pp. 403–409, 2012, doi: 10.1016/j.scient.2012.04.003.

[20] B. Omolofe and T. O. Adeloye, “Behavioral study of finite beam resting on elastic foundation and subjected to travelling distributed masses,” *Lat. Am. J. Solids Struct.*, vol. 14, no. 2, pp. 312–334, 2017, doi: 10.1590/1679-78253071.

[21] A. H. Sofiyev, S. N. Keskin, and A. H. Sofiyev, “Effects of elastic foundation on the vibration of laminated non-homogeneous orthotropic circular cylindrical shells,” *Shock Vib.*, vol. 11, no. 2, pp. 89–101, 2004, doi: 10.1155/2004/424926.

[22] A. Farshidianfar and P. Oliazadeh, “Free Vibration Analysis of Circular Cylindrical Shells: Comparison of Different Shell Theories,” *Int. J. Mech. Appl.*, vol. 2, no. 5, pp. 74–80, 2012, doi: 10.5923/j.mechanics.20120205.04.

[23] K. L. Ravisankar and K. Jeevanantham, “EXPERIMENTAL STUDY ON DIFFERENT PROPORTION OF POLYPROPYLENE FIBER IN HIGH STRENGTH CONCRETE,” pp. 2151–2156, 2021.

[24] A. K. Yadav, B. Prasad, V. Kumar, and M. Mohan, “Properties of Polypropylene Fiber Reinforced Concrete and Structural Behaviour of Beam,” *Int. J. Innov. Res. Sci. Eng. Technol.*, vol. 6, no. 6, pp. 10200–10210, 2017, doi: 10.15680/IJIRSET.2017.0606011.

[25] R. Zhang, K. Matsumoto, J. Niwa, T. Hirata, and Y. Ishizeki, “Experimental study on shear behavior of PP-ECC beams with different stirrup ratios,” *Proc. 13th East Asia-Pacific Conf. Struct. Eng. Constr. EASEC 2013*, 2013.

[26] L. M. Al-Shather, A. A. Ali, and H. M. Abed, “The Shear Behavior of Reinforced Concrete I – Beams With Polypropylene Fibers,” *Al-Nahrain J. Eng. Sci.*, vol. 20, no. 5, pp. 1040–1046, 2017.

[27] F. Altun, T. Haktanir, and K. Ari, “Effects of steel fiber addition on mechanical properties of concrete and RC beams,” *Constr. Build. Mater.*, vol. 21, no. 3, pp. 654–661, 2007, doi: 10.1016/j.conbuildmat.2005.12.006.

[28] Musitefa Adem Yimer, “Seismic Performance of Steel Fiber Reinforced Concrete Beam-Column Joints under the Variation of Column Axial Load,” *Int. J. Eng. Res.*, vol. V9, no. 02, pp. 206–224, 2020, doi: 10.17577/ijertv9is020110.

[29] O. C. Zienkiewicz, “The Finite Element Method: Its Basis and Fundamentals,” *Finite Elem. Method its Basis Fundam.*, p. iii, 2013, doi: 10.1016/b978-1-85617-633-0.00020-4.

[30] S. Khosravi and M. M. Heydari, “Design and modal analysis of gravity dams by Ansys Parametric Design Language,” *Walailak J. Sci. Technol.*, vol. 12, no. 2, pp. 167–180, 2015.

[31] I. V. Silveira and L. J. Pedroso, “Analysis of Natural Frequencies and Modes of Vibration Involving Interaction Dam-Reservoir Foundation for Concrete Gravity Dams,” *Third Int.*

Dam World Conf., no. October, pp. 1–11, 2018.

[32] O. Kessler, “Introduction to the forum,” *Rev. Int. Stud.*, vol. 38, no. 1, pp. 187–189, 2012, doi: 10.1017/S0260210511000623.

[33] I.-B. Teodoru, “Beams on Elastic Foundation. The Simplified Continuum Approach,” *Bull. Polytech. Inst. Jassy, Constr. Arch. Sect.*, vol. LV (LIX), no. 4, pp. 37–46, 2009, [Online]. Available: http://www.bipcons.ce.tuiasi.ro/Content/ArticleInformation.php?ArticleID=162.

[34] S. Limkatanyu, W. Prachasaree, N. Damrongwiriyanupap, M. Kwon, and W. Jung, “Exact stiffness for beams on Kerr-type foundation: The virtual force approach,” *J. Appl. Math.*, vol. 2013, 2013, doi: 10.1155/2013/626287.

[35] S. M. Engineering, *Department of Mechanical Engineering Modeling and Finite Element*, vol. 019. .

[36] D. Tang, G. Wu, X. Yao, and C. Wang, “Free Vibration Analysis of Circular Cylindrical Shells with Arbitrary Boundary Conditions by the Method of Reverberation-Ray Matrix,” *Shock Vib.*, vol. 2016, 2016, doi: 10.1155/2016/3814693.

[37] X. Xie, G. Jin, and Z. Liu, “Free vibration analysis of cylindrical shells using the Haar wavelet method,” *Int. J. Mech. Sci.*, vol. 77, pp. 47–56, 2013, doi: 10.1016/j.ijmecsci.2013.09.025.

[38] H. N. G. Al-Maliki, A. Al-Balhawi, A. J. H. Alshimmeri, and B. Zhang, “Structural efficiency of hollow reinforced concrete beams subjected to partial uniformly distributed loading,” *Buildings*, vol. 11, no. 9, pp. 1–16, 2021, doi: 10.3390/buildings11090391.

[39] T. W. H. Sheu, S. K. Wang, and S. F. Tsai, “Finite element analysis of particle motion in steady inspiratory airflow,” *Comput. Methods Appl. Mech. Eng.*, vol. 191, no. 25–26, pp. 2681–2698, 2002, doi: 10.1016/S0045-7825(02)00209-8.

[40] Ö. Civalek, “Nonlinear analysis of thin rectangular plates on Winkler-Pasternak elastic foundations by DSC-HDQ methods,” *Appl. Math. Model.*, vol. 31, no. 3, pp. 606–624, 2007, doi: 10.1016/j.apm.2005.11.023.